FE DYNAMIC ANALYSIS
OF
AN UMBRELLA FRAME FOR SPACE APPLICATIONS

By

Jun An Hu

February, 2006

Department of Civil Engineering and Applied Mechanics
McGill University
Montreal, Canada

A thesis submitted to the Faculty of Graduate Studies and Research in partial fulfillment of the requirements for the degree of Master of Engineering

Your file Votre référence
ISBN: 978-0-494-24966-6
Our file Notre référence
ISBN: 978-0-494-24966-6

Abstract

Deformation will occur for the flexible structures undergoing large rigid-body motion such as the opening of an umbrella, which poses a problem falling into the category of dynamics of deformable bodies, an intersected area between structural dynamics and rigid-body dynamics. Based on the Euler-Bernoulli beam theory, an FE model is developed to simulate the process of deployment of an umbrella under a zero gravity circumstance in which the structural FEA is adopted to define the displacement field of beam elements. The position of an arbitrary point on a body is located by a set of generalized coordinates of the system, including rigid and elastic sets characterizing rigid-body motion and deformation for the components, respectively. After formulating the kinetic energy, potential energy and generalized forces of the system, the governing equations of motion with different holonomic constraint conditions corresponding to the stages of the deployment are then derived by invoking Lagrange's equations with multipliers. As for the validation of this model, a rigid FE model and a continuum rigid-body model are also derived. The numeric process reveals that significant periodic vibration is induced on the leaf at full deployment if an initial velocity is applied on the sleeve of the modeled umbrella and the deformation of the members causes the retard of the deployment. Comparison of the results shows good agreement between 3-element and 6-element models, and the deformable models are validated by the rigid-body ones. Although the formulation is based on the holonomic 2-body model, it is also applicable to a more complicated nonholonomic system.

Résumé

La déformation se produira pour les structures flexibles subissant le grand mouvement d'un corps rigide tel que l'ouverture d'un parapluie, qui pose un problème entrant dans la catégorie de la dynamique des corps déformables, un secteur intersecté entre la dynamique structurale et la dynamique des corps rigides. Basé sur la théorie de poutre d'Euler-Bernoulli, un modèle d'éléments finis est développé pour simuler le déploiement d'un parapluie dans un champ de gravité nulle dans laquelle l'analyse structurale en éléments finis est adopté pour définir le réseau de déformation des éléments poutres. La position d'un point arbitraire sur un corps est localisée par un ensemble de coordonnées généralisées du système, y compris les ensembles rigides et élastiques caractérisant le mouvement d'un corps rigide et la déformation pour les composants, respectivement. Après la formulation de l'énergie cinétique, de l'énergie potentielle et des forces généralisées du système, les équations du mouvement avec différents états holonomiques de contrainte correspondant aux étapes de déploiement sont alors dérivées en utilisant les équations de Lagrange avec des multiplicateurs. Quant à la validation de ce modèle, un modèle rigide d'éléments finis et un modèle de corps rigide continu sont également dérivés. Le processus numérique indique qu'une vibration périodique significative est induite sur la feuille au plein déploiement si une première vitesse est appliquée sur la douille du parapluie modélisé et la déformation des membres cause le retard du déploiement. La comparaison des résultats montre une bonne concordance entre le modèle de 3 éléments et le modèle de 6 éléments, et les modèles déformables sont validés par ceux les modèles de corps rigides. Bien que la formulation soit basée sur le modèle holonomique à deux corps, elle est également applicable à un système nonholonomique plus complexe.

Acknowledgments

The work presented in this thesis was supervised by Professor S. C. Shrivastava to whom I'd like to give my thanks for his invaluable guidance and continuous inspiration.

To my wife, Xue Qin, I'd like to express my heartfelt gratitude for her love.

Table of Contents

List of Figures

List of Tables

List of Symbols

A_i	Cross-sectional area of body i
$[A_i]$	Transformation matrix
b	Height of the cross section
$[B_j]$	Transformation matrix
$\{C_i(\{q\})\}$	Totality of constraint equations for Case i
$[C_1], [C_2], [C_3]$	Matrix for transformation of velocities
$\{d_j\}$	Vector of node coordinates of element j
$\{e_i\}$	Elastic coordinates of body i
E_i	Modulus of elasticity of body i
$\underline{F}$	External force acting at point H
G	End point of the leaf
h , h_i	Time step
H	Joint between the sleeve and link
I_i	Area moment of inertia of body i
I_i'	Mass moment of inertia of body i
$[I]$	Identity matrix
$[J_i]$	Constraint Jacobian matrix for Case i
$[K_i], [K]$	Stiffness matrix at element and system levels
l	Length of a beam element

L	Lagrangian
l_i	Dimensions of the system
$[Mc]$	Mixed mass matrix of the system
M_i	Moment at an arbitrary point on element j of body i
$[M_i]$, $[M]$	Mass matrices at element and system levels
$[N]$	Shape function of beam element
$\{p\}$	Position of a point in undeformed status
$\{q\}$	Vector of generalized coordinates for the system
$\{q_F\}$	Position at the end of first stage
$\{q_H\}$	Initial position for the second stage
$\{q_i\}$	Vector of generalized coordinates for body i
$\{Q^{appl.nc}\}$	Generalized nonconservative forces of the system
$\{Q\}$	Mixed generalized forces
$\underline{r}$	Position vector of an arbitrary point on element
$\underline{R}_i$	Position vector of the origin of moving frame i
R_i^x, R_i^y	Components of $\underline{R}_i$
S	Position of H at full deployment of an umbrella
t	Time
T_i, T	Kinetic energy at element and system levels
u, v	Axial and transverse displacement field of an element
u_i , v_i	Displacements of node i of a beam element

$\{\overline{u}\}$	Total displacement field of an element
$\{\overline{\overline{u}}\}$	Location of a point in a moving frame
V_i, V	Potential energy at element and system levels
V_0	Input velocity at joint H
xy	Coordinate system of a beam element
XOY	Inertial frame
$X'O'Y'$	The moving frame fixed on the leaf
$X''O''Y''$	The moving frame fixed on the link
X_i	Abscissa of node i of element i measured in moving frame
α_0	Initial value of α_1
α_i	Orientation of the moving frame i
θ_i	Rotation of node i of a beam element
η	Variable of shape function $\eta = \frac{x}{l}$
ρ_i	Mass per unit length of body i
Φ_i	Constraint equation i
$\{\lambda\}$	Vector of Lagrangian multipliers
ϵ_c	Constraint error tolerance
ε	Strain
σ	Stress

Superscripts:

T	Transpose of a matrix

Matrix symbols:

$\{\ \}$	Column matrix
$\langle\ \rangle$	Row matrix
$[\ ]$	Rectangular matrix

Chapter 1

Introduction

1. 1 Background

The deployment of packed deformable structures such as a membrane antenna in a zero gravity space environment can be characterized as a motion of high speed and light mass, in which the structures experience not only large rigid-body translation and rotation but also elastic deformation at a certain level. In this case, the traditional rigid-body assumption is no longer applicable in light of the considerable deformation that may threaten the intended functions of the structures. The reasonable way to simulate the process of deployment is an intersection between rigid-body dynamics and structural dynamics, in which Lagrange's equation is used to develop the governing equations of motion. These equations always display highly nonlinear behavior because there exist the following inertial couplings:

(a) couplings between elastic deformation and rigid-body translation;

(b) couplings between elastic deformation and rigid-body rotation;

(c) couplings between rigid-body translations and rotation.

The formulations for the system with small deformation can be categorized into a distributed parameter model and a discretized parameter model with corresponding strategies of solution.

1. 1. 1 The distributed parameter model

The distributed parameter formulation treats the pertinent components of the system as continuum bodies with distributed mass and flexibility. The independent generalized coordinates or constrained generalized coordinates can be adopted to describe the kinematic and dynamic aspects for each body and the whole system. Methods of

analytical mechanics such as Lagrange's equation and Jourdain's principle are applied to derive the governing equations of motion in the form of partial differentiation for the case of the independent generalized coordinates or algebraic-partial differentiation for the constrained generalized coordinates.

This is often referred to as boundary-value problems with prescribed boundary conditions. For a complex system it is difficult or impossible to find the closed-form solutions because of the aforementioned couplings. So efforts have been concentrated on the discretization of the derived equations to transform them into ordinary differential ones by an approximate Galerkin method. Therefore, we can obtain the discretized solutions to these closed-form equations. However, as we can see that fewer variables are involved in the equations of motion compared with the discretized formulations, they can provide a clear insight into the dynamic behavior of the system.

1. 1. 2 The discretized parameter model

The discretized parameter formulations include the assumed modes method and the finite element method. For the first method, the elastic displacement of an arbitrary point on a body is approximated by a series constituted from a linear combination of mode functions multiplied by time-dependent mode coordinates in a body-fixed frame. The mode functions can be found by solving the frequency equation of the body corresponding to specified boundary conditions or by experiment. Then we can express the position, velocity, and acceleration of that point with respect to the global coordinate system, and hence kinetic and potential energy of the body with these mode coordinates and other generalized coordinates related to the rigid-body motion. Once the totalities of the kinetic energy and the potential energy are computed, Lagrange's equation is invoked to derive the governing equations of motion for the system in the form of ordinary differentiation, or algebraic ordinary differentiation if Lagrangian multipliers are introduced.

The formulation of the finite element method is to discretize each component of the system by a number of compatible elements and express the displacement field of deformation for an element with shape functions and nodal coordinates of the element according to FEA. Similarly, we can then describe the kinematic aspects of any point on the element, and calculate the kinetic and potential energy of the element with nodal coordinates of the element, and the generalized coordinates representing the rigid-body translation and rotation of the body, on which the element is attached. While the summations of the kinetic energy and the potential energy of all elements are derived with respect to generalized coordinates of the system, the mass matrix and stiffness matrix for the bodies and the whole system can be assembled from those of the elements. By resorting to Lagrange's equation, we can finally arrive at the governing equations of motion, also in the form of ordinary differentiation.

The method of direct numerical integration can be used to solve these differential or differential-algebraic equations.

1. 2 Description of the intended work

The objective of this research work is to develop an FE model to simulate the opening of an umbrella with straight ribs and two hinges on each rib in a zero gravity environment, which is deemed as the first step toward refined modeling of real space structures. The dynamic analysis will determine the induced stresses in the process of deployment and ensuing vibrations after the full deployment.

There are seven chapters in this thesis. The second chapter is the literature review, which gives brief descriptions of the previous research related to this field. In Chapter 3, the physical model of an umbrella is first developed and the discussion is made on how to configure the coordinate systems necessary to describe the motion of a deformable body. Then the displacement field of a beam element defined by structural FEA is introduced to

locate an arbitrary point on an element of the body in the inertial frame using the vector of generalized coordinates of the body, which consists of rigid and elastic ones.

Chapter 4 details the procedure to derive the differential-algebraic equations of motion by following the method of constrained Lagrangian dynamics. It is shown that the assembled mass matrix of the system is a function of the generalized coordinates of the system and the generalized forces are dependent on both the generalized coordinates and the generalized velocities of the system, all of which contribute to the nonlinearity of the equations of motion, while the stiffness matrix of the system remains constant. In this chapter, different constraint conditions and the corresponding Jacobian matrices are discussed in accordance with the process of deployment, the full deployment, and the rigid-body mode, respectively. As for the validation of the finite element models the formulation of rigid-body dynamics is briefly dealt with in the last section of this chapter.

In Chapter 5, the strategy of solution is outlined and the conservation of energy is assumed to develop the initial velocities when the ensuing vibrations at the full deployment are analyzed. The numerical results and discussions are carried out in Chapter 6 and the thesis ends with concluding remarks on the main findings of the research and recommendation for further studies, in Chapter 7.

Chapter 2

Literature Review

As mentioned previously, the problem of the deployment of an umbrella falls into the dynamics of flexible structures experiencing large rigid-body motion, which is a hybridized area between rigid-body dynamics and structural dynamics. Many scientists and engineers have been putting efforts into this field and the achievements can be found in a large body of literature in which the methods can be categorized into the distributed parameter formulation and the discretized parameter formulation.

2. 1 The distributed parameter formulation

The distributed parameter formulation has been detailed by K. H. Low and his coworkers [9], Jorge Martins and the coworkers [11], B.V. Viscomi et al. [12], J. C. Simo and L. Vu-Quoc [16], and J. Kövecses [23]. K. H. Low and co-workers have derived dynamic equations for manipulators with both rigid and flexible links using Hamilton's principle, but without giving solutions. Jorge Martins and coworkers have developed a model of a planar manipulator with one flexible link in which the centrifugal stiffening effect caused by the rotation of the link is considered and the solutions are given by discretization. B. V. Viscomi et al. have analyzed the bending response of a flexible link of a slider-crank mechanism by energy methods and have utilized the Galerkin technique to solve the governing equations of motion. J. C. Simo and L. Vu-Quoc have proposed an approach, based on the finite strain rod theories, capable of dealing with the finite rotations to derive simpler dynamic equations than those formulated by the conventional floating frame of reference; and the Galerkin method of discretization is used similarly in the numerical examples. J. Kövecses has developed a

three-dimensional model for the kinematic and dynamic analysis of flexible robots by using Jourdain's principle.

2. 2 The discretized parameter formulation

The discretized parameter formulation includes the assumed modes method and the finite element method. By resorting to the assumed modes method, Alessandro De Luca [10] has derived the equations of motion for planar lightweight robot arms with multiple flexible links that are modeled as Euler-Bernoulli beams with proper clamped-mass boundary conditions. In the same way, R. A. Laskin et al.[13] have developed the ordinary differential equations of motion for a free-free beam experiencing large overall motions by invoking Kane's equations, and special attention is given to the effects of rotation about the geometrical stiffening. M. Benati and A. Morro [22] have presented a dynamic model for a chain with flexible links using the Lagrangian formulation.

As for the finite element method, Ji Oh Song and Edward J. Haug [15] have developed an FE model for the planar mechanisms with flexible members using the Lagrangian constrained generalized coordinates in which the origins of the body-fixed coordinate systems are fixed at the centroids of members and small elastic deformation is assumed. I. Sharf [17] has discussed the problems caused by the linearization of displacement when dealing with the large-deformation dynamics using the explicit nonincremental, nonlinear beam elements and suggests that the incremental approach is not suitable for a dynamic simulation. R. G. Langlois and R. J. Anderson [19] have proposed a formulation for the open and loop mechanisms with joint flexible bodies based on Kane's equation, taking into account the nonlinear deformation and geometric stiffening effects. P. B. Usoro and co-workers [24] have developed an FE model for a two-link manipulator system based on the Lagrangian formulation.

Rex J. Theodore and Ashitava Ghosal [8] have presented the results of a comparison between the assumed modes and the finite element methods and recommend

that the assumed modes method be used for the uniform cross-section as well as for the single-link flexible manipulators, while the finite element formulation should be used for the complex cross-section and for the multilink flexible system. Madeleine Pascal [18] points out the ways to select the floating frame and how to introduce the geometric stiffening effect for the slender members. Ahmed A. Shabana [7, 20] has given detailed information about the formulations utilized in multibody dynamics and advocates that the floating frame of reference apply in the case of small deformation and the absolute nodal coordinate formulation for large deformation.

For the knowledge of structural FEA, structural dynamics, and rigid-body dynamics, we can refer to the pertinent books [1], [3, 14, 21] and [4, 5, 6], respectively. For analytical mechanics, H. Baruh [2] has presented a detailed explanation of how to select the body-fixed frame and the way to count the geometric stiffening effects.

For the purposes of this thesis, the floating frame of reference and the more straightforward formulation of constrained Lagrangian dynamics are adopted to simulate the opening process of an umbrella in which only the small deformation is taken into account.

Chapter 3

Physical Model and Location of Points of FE Model

3. 1 Development of physical model

An ordinary umbrella is usually composed of a folding frame on which a canopy is attached and one axle that ends in a handle. The folding frame consists of an even number of sets of hinged leafs and links axisymmetrically distributed about the axle and a sliding sleeve joint by these links. The umbrella is opened and closed with the sleeve moving up and down along the axle.

In order to analyze the dynamic behavior in the deployment of an umbrella we have to develop a simplified physical model expedient to simulate this process. Considering the characteristics of axisymmetry of geometry and elastic properties of an umbrella, the loads and the boundary conditions, we can change this spatial structure into a planar mechanism made up of one leaf and one link hinged at point O'' without the fabric as shown in Figure 3.1.

The sleeve symbolized as a slider joint at point H of the link can only move in the trajectory of the center line of the axle represented by the dash-dot line and stop at point S when full deployment is reached. The leaf can rotate about the point O' fixed on the center line.

In this physical model the mass of the sleeve is neglected and the damping, frictional and temperature effects are also ignored. We further assume only small deformation is produced in the deployment of the umbrella and treat the leaf and link as uniform beams. So the Euler-Bernoulli beam theory is applicable here in which shear effect and inertia of rotation are neglected. The displacement field of an element considers both longitudinal and transverse deformations. The kinetic energy comes from both rigid-body motion and elastic deformation while the potential energy originates only

from the elastic deformation (so-called strain energy) because the gravity is negligible in space.

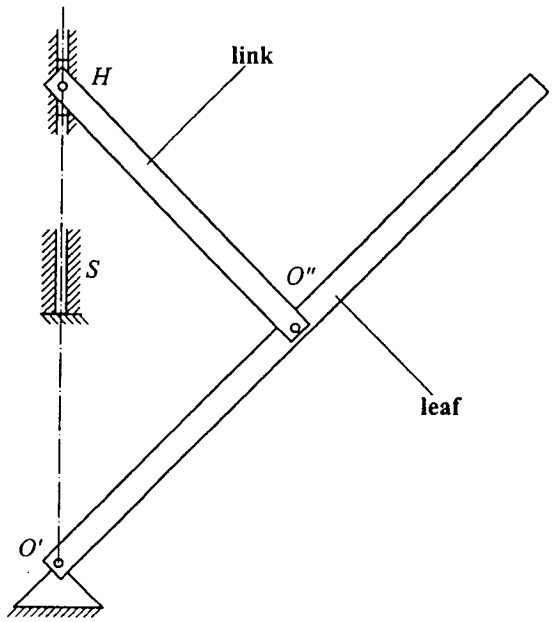

Figure 3.1 The physical model of an umbrella

3. 2 Configuration of the coordinate systems

This model takes into account both the in-plane rigid-body displacements and small elastic deformation of the bodies. To simulate the dynamic behavior of a deformable beam by finite element method we need to use the three sets of coordinate systems shown in Figure 3.2. The inertial frame XOY is fixed and acts as a uniform reference base for rigid-body motion of each body and constraint relationships between bodies of the system. The moving frame $X'O'Y'$ attached on a beam in undeformed status divides the motion of a body into rigid-body mode and elastic deformation, which can be formulated by the finite element method. So it functions as a measurement base for the deformation of the body and compatibility of elements meshed on the body. The third frame is the element coordinate system xy that describes the displacements of the points

on the element i with node i and node j. The axes of the element coordinate systems are parallel to those of the moving frame and are fixed relative to it.

The origin and orientation of the moving frame can be located by vector $\underline{R}$ and angle α respectively. The origin of the element coordinate system of element i on the beam is measured by X_i in the moving frame. To define the position of an arbitrary point Q' on element i one has to find the undeformed position measured by x and the displacement $\overline{u}$ of that point with respect to the element coordinate system xy.

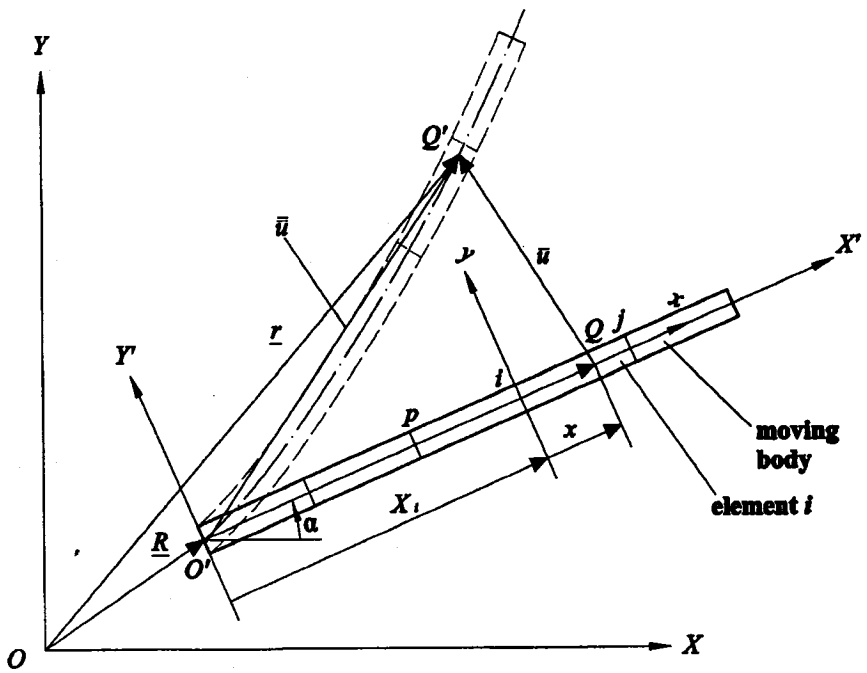

Figure 3.2 Coordinate systems for a moving deformable beam

3. 3 Displacement field of a beam element

Figure 3.3 shows the displacement components of node i and node j of a uniform beam element i mentioned in Figure 3.2, in which u, v and θ represent the axial and transverse displacements, and the rotation or slope at corresponding node, respectively.

We assume that the axial and transverse displacements between node i and node j are respectively approximated linearly and cubically as follows:

$$u = (1-\eta)u_i + \eta u_j \tag{3.1}$$

$$v = (1-3\eta^2+2\eta^3)v_i + l(\eta-2\eta^2+\eta^3)\theta_i + (3\eta^2-2\eta^3)v_j + l(\eta^3-\eta^2)\theta_j \tag{3.2}$$

in which $\eta = \frac{x}{l}$, and l is the length of element i.

In matrix format, we obtain

$$\{\bar{u}\} = [N]\{d\} \tag{3.3}$$

where $\{\bar{u}\} = \begin{Bmatrix} u \\ v \end{Bmatrix}$,

and $[N]$ is the shape function,

$$[N] = \begin{bmatrix} 1-\eta & 0 & 0 & \eta & 0 & 0 \\ 0 & 1-3\eta^2+2\eta^3 & l(\eta-2\eta^2+\eta^3) & 0 & 3\eta^2-2\eta^3 & l(\eta^3-\eta^2) \end{bmatrix} \tag{3.4}$$

$\{d\}$ is the column vector of node coordinates of element i,

$$\{d\} = \langle u_i \;\; v_i \;\; \theta_i \;\; u_j \;\; v_j \;\; \theta_j \rangle^T \tag{3.5}$$

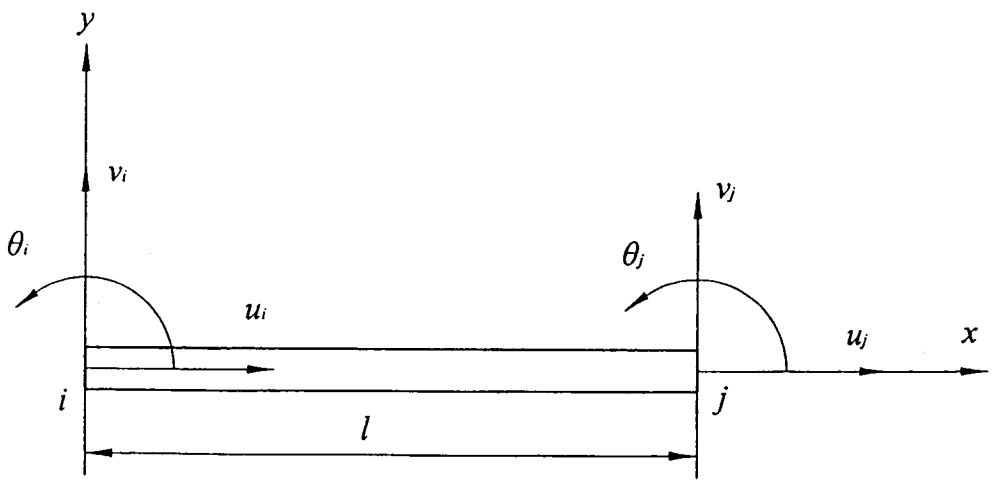

Figure 3.3 Beam element

3.4 Definition of the position of an arbitrary point on an element

Now we can decide the position of an arbitrary point on element i of the beam in the inertial frame by a vector $\underline{r}$,

$$\begin{aligned}\underline{r} &= \underline{R} + [A](\{p\} + \{\bar{u}\}) \\ &= \underline{R} + [A]\{\bar{\bar{u}}\}\end{aligned} \tag{3.6}$$

where

Vector $\underline{R}$ locates the origin of the moving frame, and $\underline{R} = \begin{Bmatrix} R^x \\ R^y \end{Bmatrix}$,

$[A]$ is the transformation matrix from the moving frame to the inertial frame,

$$[A] = \begin{bmatrix} \cos\alpha & -\sin\alpha \\ \sin\alpha & \cos\alpha \end{bmatrix}$$

$\{p\}$ is the position of the point in undeformed status and

$$\{p\} = \begin{Bmatrix} X_i + x \\ 0 \end{Bmatrix}$$

in which

X_i is the abscissa of node i of element i measured in the moving frame,

x is the abscissa of the concerned point measured in the local element coordinate system xy.

The ordinate of the point is zero because we assume that both the X'-axis of the moving frame and x-axes of the element coordinate systems coincide with the center line of the uniform beam.

$\{\bar{\bar{u}}\}$ is the position of the point in deformed status with respect to the moving frame and

$$\{\bar{\bar{u}}\} = \{p\} + \{\bar{u}\} \tag{3.7}$$

The geometrical expressions of vectors $\{p\}$, $\{\bar{u}\}$, $\{\bar{\bar{u}}\}$ and $\underline{r}$ are shown in Figure 3.2.

3. 5 Application to the model

Figure 3.4 shows the slider at point H of the link can only move in the trajectory along the Y-axis of the inertial frame. The leaf can rotate about the point $O(O')$, the origins of the inertial frame XOY, and the moving frame $X'O'Y'$ that is fixed on the leaf with the point O'' on its X'-axis. The other moving frame $X''O''Y''$ is attached to the link with its origin at the joint O'' and with its X''-axis passing through the point H.

Both the leaf and the link are deemed uniform beams with corresponding geommetric and material characteristics. To clearly describe the process of formulation, we place two beam elements on the leaf and one element on the link, which can be easily followed by more densely meshed finite element models.

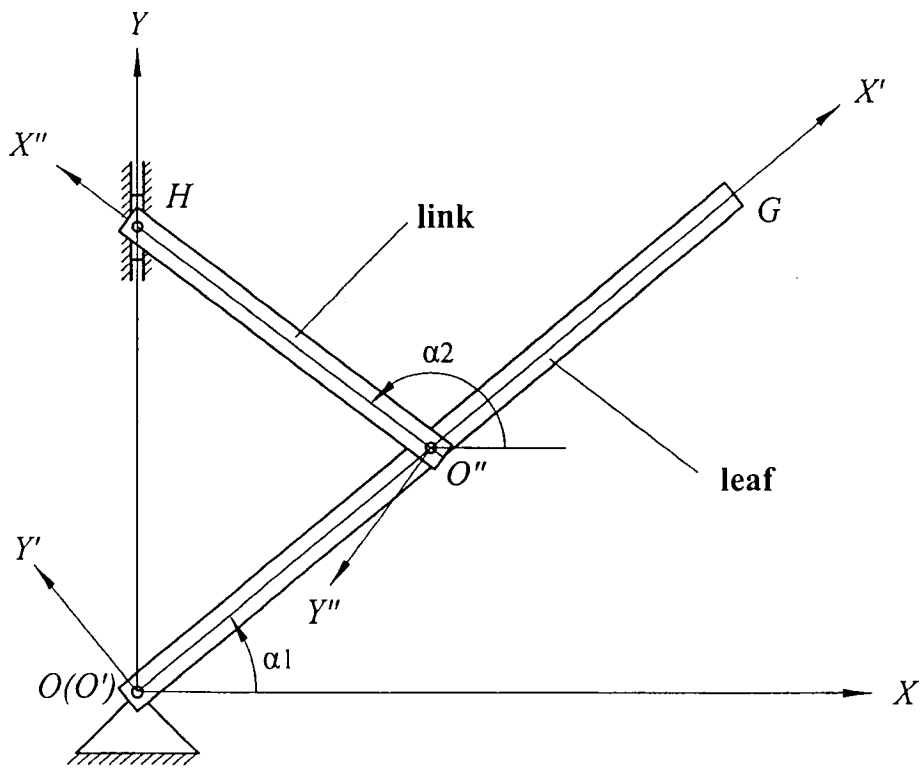

Figure 3.4 Configuration of the model

The two elements on the leaf are divided by nodes 1, 2 and 3 at points $O(O')$, O'' and G respectively, as shown in Figure 3.5 . The displacement components of those nodes form the vector

$$\{e_1\} = \langle\, u_1 \quad v_1 \quad \theta_1 \quad u_2 \quad v_2 \quad \theta_2 \quad u_3 \quad v_3 \quad \theta_3 \rangle^T \tag{3.8}$$

which describes the elastic deformation of the leaf.

However, the moving frame $X'O'Y'$ attached on the leaf passing through the origin O'(node 1) and the joint O''(node 2) means additional constraints are introduced:

$$u_1 = v_1 = v_2 = 0 \tag{3.9}$$

which guarantees that no rigid-body mode exists in the moving frame.

Considering equation 3.9, equation 3.8 reduces to

$$\{e_1\} = \langle\, \theta_1 \quad u_2 \quad \theta_2 \quad u_3 \quad v_3 \quad \theta_3 \rangle^T \tag{3.10}$$

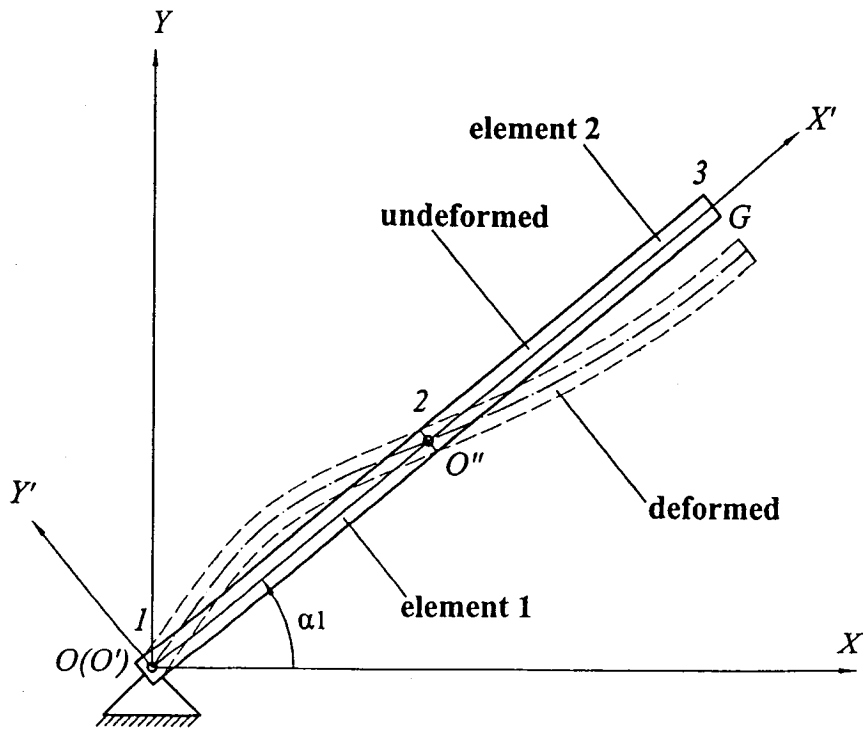

Figure 3.5 Configuration of the leaf

Then the vector of node coordinates of element 1 and 2 on the leaf can be expressed by vector $\{e_1\}$ as

$$\{d_1\} = \langle 0 \quad 0 \quad \theta_1 \quad u_2 \quad 0 \quad \theta_2 \rangle^T$$
$$= [B_1]\{e_1\} \tag{3.11}$$
$$\{d_2\} = \langle u_2 \quad 0 \quad \theta_2 \quad u_3 \quad v_3 \quad \theta_3 \rangle^T$$
$$= [B_2]\{e_1\} \tag{3.12}$$

in which $[B_1]$ and $[B_2]$ are transformation matrices:

$$[B_1] = \begin{bmatrix} 0 & 0 & 0 & 0 & 0 & 0 \\ 0 & 0 & 0 & 0 & 0 & 0 \\ 1 & 0 & 0 & 0 & 0 & 0 \\ 0 & 1 & 0 & 0 & 0 & 0 \\ 0 & 0 & 0 & 0 & 0 & 0 \\ 0 & 0 & 1 & 0 & 0 & 0 \end{bmatrix} \text{ and } [B_2] = \begin{bmatrix} 0 & 1 & 0 & 0 & 0 & 0 \\ 0 & 0 & 0 & 0 & 0 & 0 \\ 0 & 0 & 1 & 0 & 0 & 0 \\ 0 & 0 & 0 & 1 & 0 & 0 \\ 0 & 0 & 0 & 0 & 1 & 0 \\ 0 & 0 & 0 & 0 & 0 & 1 \end{bmatrix}.$$

Similarly for the link in Figure 3.6, if there is only one element on it with nodes 4 and 5 at points O'' and H respectively, the deformation vector can be found as

$$\{e_2\} = \langle \ \theta_4 \ u_5 \ \ \theta_5 \ \rangle^T \tag{3.13}$$

because of the constraints

$$u_4 = v_4 = v_5 = 0$$

So the vector of node coordinates of the element on the link is

$$\{d_3\} = \langle 0 \quad 0 \quad \theta_4 \quad u_5 \quad 0 \quad \theta_5 \rangle^T$$
$$= [B_3]\{e_2\} \tag{3.14}$$

in which

$$[B_3] = \begin{bmatrix} 0 & 0 & 0 \\ 0 & 0 & 0 \\ 1 & 0 & 0 \\ 0 & 1 & 0 \\ 0 & 0 & 0 \\ 0 & 0 & 1 \end{bmatrix}.$$

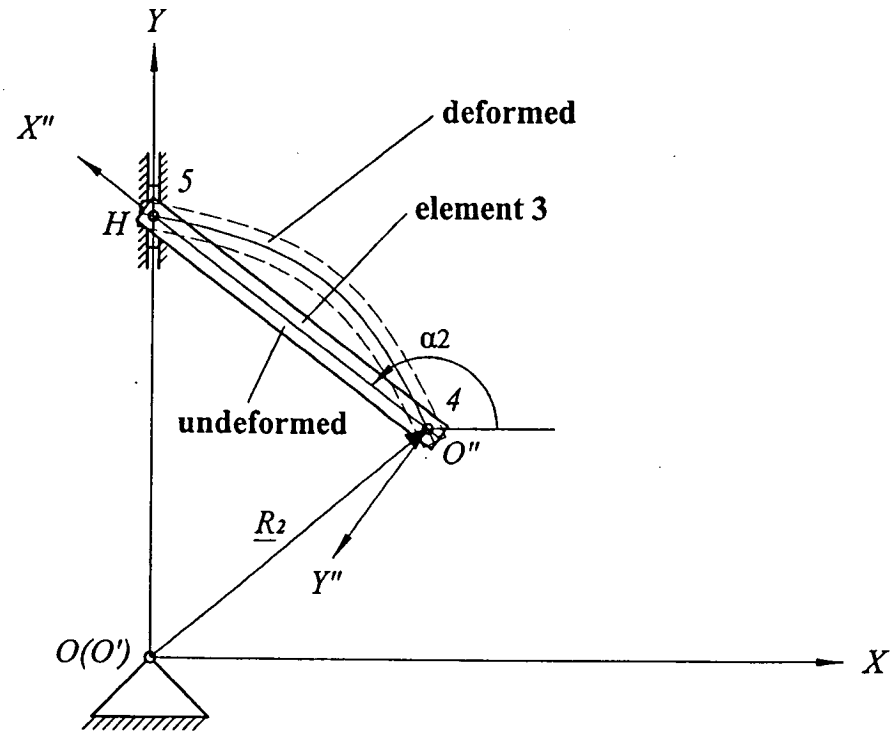

Figure 3.6 Configuration of the link

In general form, the vector of node coordinates of the element j on body i can be expressed as

$$\{d_j\} = [B_j]\{e_i\} \tag{3.15}$$

where

$$i = \begin{cases} 1 & \text{for the leaf, and then } j = 1, 2. \\ 2 & \text{for the link, and then } j = 3. \end{cases}$$

Considering equation 3.15, equation 3.3 and equation 3.6 become

$$\begin{aligned} \{\overline{u}_j\} &= [N]\{d_j\} \\ &= [N][B_j]\{e_i\} \end{aligned} \tag{3.16}$$

and

$$\begin{aligned} \underline{r}_i &= \underline{R}_i + [A_i]\{\overline{\overline{u}}_j\} \\ &= \underline{R}_i + [A_i](\{p_j\} + [N][B_j]\{e_i\}) \end{aligned} \tag{3.17}$$

where

$$[A_i] = \begin{bmatrix} \cos\alpha_i & -\sin\alpha_i \\ \sin\alpha_i & \cos\alpha_i \end{bmatrix} \text{ and } \{p_j\} = \begin{Bmatrix} X_j + x \\ 0 \end{Bmatrix}$$

From this expression we may conclude that $\underline{R}_i$, α_i and $\{e_i\}$ are enough to locate an arbitrary point on element j of body i in the inertial frame. So we can form a vector of generalized coordinates by them for the body i as

$$\{q_i\} = \begin{Bmatrix} \underline{R}_i \\ \alpha_i \\ e_i \end{Bmatrix} \tag{3.18}$$

with the size of $3(n_i + 1)$ by 1, and n_i is the number of elements on body i. In vector $\{q_i\}$, $\underline{R}_i$ and α_i are called rigid coordinates that relate to rigid-body motion, while $\{e_i\}$ is named elastic coordinates concerning deformation of body i. These two sets of coordinates can be utilized to complete the formulation of FEA conveniently.

For the leaf, $n_1 = 2$, so there are 9 parameters in vector $\{q_1\}$:

$$\{q_1\} = \langle R_1^x \;\; R_1^y \;\; \alpha_1 \;\; \theta_1 \;\; u_2 \;\; \theta_2 \;\; u_3 \;\; v_3 \;\; \theta_3 \rangle^T \tag{3.19}$$

Considering that the point O', origin of the moving frame $X'O'Y'$, is coincided with the origin of the inertial frame XOY, we arrive at,

$$R_1^x = R_1^y = 0 \tag{3.20}$$

and equation 3.19 is reduced to

$$\{q_1\} = \langle \alpha_1 \;\; \theta_1 \;\; u_2 \;\; \theta_2 \;\; u_3 \;\; v_3 \;\; \theta_3 \rangle^T \tag{3.21}$$

Corresponding to the leaf, equation 3.17 becomes

$$\begin{aligned} \underline{r}_1 &= [A_1]\{\overline{\overline{u}}_j\} \\ &= [A_1](\{p_j\} + [N][B_j]\{e_1\}) \qquad\qquad j = 1, 2 \end{aligned} \tag{3.22}$$

which locates an arbitrary point on element 1 or element 2.

Similarly, 6 parameters exist in $\{q_2\}$ for the link:

$$\{q_2\} = \langle R_2^x \;\; R_2^y \;\; \alpha_2 \;\; \theta_4 \;\; u_5 \;\; \theta_5 \rangle^T \tag{3.23}$$

and

$$\begin{aligned}\underline{r}_2 &= \underline{R}_2 + [A_2]\{\overline{\overline{u}}_3\} \\ &= \underline{R}_2 + [A_2](\{p_3\} + [N][B_3]\{e_2\})\end{aligned} \tag{3.24}$$

which locates an arbitrary point on element 3.

Therefore, a vector with 13 components can describe the motion of the system, and can be expressed as

$$\{q\} = \langle \alpha_1 \;\; \theta_1 \;\; u_2 \;\; \theta_2 \;\; u_3 \;\; v_3 \;\; \theta_3 \;\; R_2^x \;\; R_2^y \;\; \alpha_2 \;\; \theta_4 \;\; u_5 \;\; \theta_5 \rangle^T \tag{3.25}$$

Chapter 4

Derivation of the Equations of Motion for the System

4. 1 Kinetic energy of the system

Once the position of a material point of the body is decided, one can find the velocity of that point by differentiation and thus formulate the kinetic energy of the system.

Based on the Euler-Bernoulli beam theory, the shear effect and the rotary inertia of the cross section will be ignored. Therefore, the kinetic energy of element j on body i can be expressed as

$$T_j = \frac{1}{2}\int_0^l \rho_i \, \underline{\dot{r}}_i \cdot \underline{\dot{r}}_i dx \qquad j = 1,2,3;\ i = 1,2 \qquad (4.1)$$

in which ρ_i is mass per unit length of body i and l is the length of the element.

Detailed expression of kinetic energy for each element is discussed as follows:

Differentiating both sides of equation 3.22 with respect to time t leads to

$$\begin{aligned} \underline{\dot{r}}_1 &= [\dot{A}_1]\{\bar{\bar{u}}_1\} + [A_1]\{\dot{\bar{\bar{u}}}_1\} \qquad (j=1) \\ &= [C_1]\{\dot{q}_1\} \end{aligned} \qquad (4.2)$$

where

$$[C_1] = \left[\, [A_1']\{\bar{\bar{u}}_1\} \quad [A_1][N][B_1] \,\right] \qquad (4.3)$$

and

$$\{\dot{q}_1\} = \begin{Bmatrix} \dot{\alpha}_1 \\ \dot{e}_1 \end{Bmatrix} \qquad (4.4)$$

which is the generalized velocity vector of the leaf. The dot means differentiation with respect to time t, while prime represents partial differentiation with respect to α_1.

$$[A_1'] = \begin{bmatrix} -\sin\alpha_1 & -\cos\alpha_1 \\ \cos\alpha_1 & -\sin\alpha_1 \end{bmatrix} \qquad (4.5)$$

Substituting equation 4.2 into the equation 4.1, we get the kinetic energy of element 1:

$$T_1 = \frac{1}{2}\{\dot{q}_1\}^T\left(\int_0^{l_1}\rho_1[C_1]^T[C_1]dx\right)\{\dot{q}_1\}$$
$$= \frac{1}{2}\{\dot{q}_1\}^T[M_1]\{\dot{q}_1\} \tag{4.6}$$

where $[M_1]$ is the mass matrix of element 1,

$$[M_1] = \int_0^{l_1}\rho_1[C_1]^T[C_1]dx \tag{4.7}$$

and l_1 is the length of element 1.

By referring to equation 4.3 and considering $X_1 = 0$ for element 1, $[M_1]$ can be partitioned as the following submatrices:

$$M_1(1,1) = \rho_1 l_1\left(\frac{1}{3}l_1^2 + \frac{2}{3}l_1u_2 + \frac{1}{105}l_1^2\theta_1^2 - \frac{1}{70}l_1^2\theta_1\theta_2 + \frac{1}{3}u_2^2 + \frac{1}{105}l_1^2\theta_2^2\right) \tag{4.8}$$

with a size of 1 by 1.

$M_1(1,2)$ is the coupling term between rotation and deformation,

$$M_1(1,2) = \rho_1 l_1^2\left\langle \frac{1}{30}(l_1+u_2) \quad -\frac{1}{30}\theta_1 + \frac{1}{20}\theta_2 \quad -\frac{1}{20}(l_1+u_2) \quad 0 \quad 0 \quad 0\right\rangle \tag{4.9}$$

with a size of 1 by 6.

$$M_1(2,2) = \rho_1 l_1\begin{bmatrix} \frac{1}{105}l_1^2 & 0 & -\frac{1}{140}l_1^2 & 0 & 0 & 0 \\ 0 & \frac{1}{3} & 0 & 0 & 0 & 0 \\ -\frac{1}{140}l_1^2 & 0 & \frac{1}{105}l_1^2 & 0 & 0 & 0 \\ 0 & 0 & 0 & 0 & 0 & 0 \\ 0 & 0 & 0 & 0 & 0 & 0 \\ 0 & 0 & 0 & 0 & 0 & 0 \end{bmatrix} \tag{4.10}$$

with size 6 by 6.

By symmetry,

$$M_1(2,1) = M_1(1,2)^T = \rho_1 l_1^2 \begin{pmatrix} \frac{1}{30}(l_1+u_2) \\ -\frac{1}{30}\theta_1 + \frac{1}{20}\theta_2 \\ -\frac{1}{20}(l_1+u_2) \\ 0 \\ 0 \\ 0 \end{pmatrix} \tag{4.11}$$

A full picture of $[M_1]$ is shown in Appendix A.

Similarly, the kinetic energy of element 2 can be formulated as:

$$\begin{aligned} T_2 &= \frac{1}{2}\{\dot{q}_1\}^T\Big(\int_0^{l_2}\rho_1[C_2]^T[C_2]dx\Big)\{\dot{q}_1\} \\ &= \frac{1}{2}\{\dot{q}_1\}^T[M_2]\{\dot{q}_1\} \end{aligned} \tag{4.12}$$

where $[M_2]$ is the mass matrix of element 2, and

$$[M_2] = \int_0^{l_2}\rho_1[C_2]^T[C_2]dx \tag{4.13}$$

$$[C_2] = \Big[\,[A_1']\{\overline{\overline{u}}_2\} \quad [A_1][N][B_2]\Big] \tag{4.14}$$

and $l_2$is the length of element 2.

By considering $X_1 = l_1$ for element 2, the submatrices of $[M_2]$ can be derived as

$$\begin{aligned} M_2(1,1) = \\ &\rho_1 l_2\Big(l_1^2 + l_1l_2 + \frac{1}{3}l_2^2 + l_1u_2 + \frac{1}{3}l_2u_2 + l_1u_3 + \frac{2}{3}l_2u_3 \\ &+ \frac{1}{3}u_2^2 + \frac{1}{3}u_2u_3 + \frac{1}{105}l_2^2\theta_2^2 + \frac{13}{210}l_2\theta_2v_3 - \frac{1}{70}l_2^2\theta_2\theta_3 \\ &+ \frac{1}{3}u_3^2 + \frac{13}{35}v_3^2 - \frac{11}{105}l_2v_3\theta_3 + \frac{1}{105}l_2^2\theta_3^2\Big) \end{aligned} \tag{4.15}$$

and $M_2(1,2)$ is the coupling term between rotation and deformation,

$$\begin{aligned} M_2(1,2) = \\ &\rho_1 l_2\langle 0, -\frac{1}{60}(3l_2\theta_2 + 9v_3 - 2l_2\theta_3), \frac{1}{60}l_2(2l_2 + 5l_1 + 3u_2 + 2u_3), \\ &-\frac{1}{60}(2l_2\theta_2 + 21v_3 - 3l_2\theta_3), \frac{1}{20}(7l_2 + 10l_1 + 3u_2 + 7u_3), \\ &-\frac{1}{60}l_2(3l_2 + 5l_1 + 2u_2 + 3u_3)\rangle \end{aligned} \tag{4.16}$$

with size 1 by 6.

$$M_2(2,2) = \rho_1 l_2 \begin{bmatrix} 0 & 0 & 0 & 0 & 0 & 0 \\ 0 & \frac{1}{3} & 0 & \frac{1}{6} & 0 & 0 \\ 0 & 0 & \frac{1}{105}l_2^2 & 0 & \frac{13}{420}l_2 & -\frac{1}{140}l_2^2 \\ 0 & \frac{1}{6} & 0 & \frac{1}{3} & 0 & 0 \\ 0 & 0 & \frac{13}{420}l_2 & 0 & \frac{13}{35} & -\frac{11}{210}l_2 \\ 0 & 0 & -\frac{1}{140}l_2^2 & 0 & -\frac{11}{210}l_2 & \frac{1}{105}l_2^2 \end{bmatrix} \tag{4.17}$$

with size 6 by 6.

By symmetry,

$$M_2(2,1) = M_2(1,2)^T = \rho_1 l_2 \begin{pmatrix} 0 \\ -\frac{1}{60}(3l_2\theta_2 + 9v_3 - 2l_2\theta_3) \\ \frac{1}{60}l_2(2l_2 + 5l_1 + 3u_2 + 2u_3) \\ -\frac{1}{60}(2l_2\theta_2 + 21v_3 - 3l_2\theta_3) \\ \frac{1}{20}(7l_2 + 10l_1 + 3u_2 + 7u_3) \\ -\frac{1}{60}l_2(3l_2 + 5l_1 + 2u_2 + 3u_3 \end{pmatrix} \tag{4.18}$$

$[M_2]$ is displayed in Appendix A.

For element 3, differentiating both sides of equation 3.24 with respect to time t leads to

$$\begin{aligned} \dot{\underline{r}}_2 &= \dot{\underline{R}}_2 + [\dot{A}_2]\{\bar{\bar{u}}_3\} + [A_2]\{\dot{\bar{\bar{u}}}_3\} \\ &= [C_3]\{\dot{q}_2\} \end{aligned} \tag{4.19}$$

where

$$[C_3] = \begin{bmatrix} I & [A_2']\{\bar{\bar{u}}_3\} & [A_2][N][B_3] \end{bmatrix} \tag{4.20}$$

in which $[I]$ is the identity matrix of 2 by 2, and

$$\{\dot{q}_2\} = \begin{Bmatrix} \dot{\underline{R}}_2 \\ \dot{\alpha}_2 \\ \dot{e}_2 \end{Bmatrix} \tag{4.21}$$

which is the generalized velocity vector of the link.

and

$$[A_2'] = \begin{bmatrix} -\sin\alpha_2 & -\cos\alpha_2 \\ \cos\alpha_2 & -\sin\alpha_2 \end{bmatrix} \tag{4.22}$$

Substituting equation 4.19 into the equation 4.1, we get the kinetic energy of element 3:

$$T_3 = \frac{1}{2}\{\dot{q}_2\}^T\left(\int_0^{l_3}\rho_2[C_3]^T[C_3]dx\right)\{\dot{q}_2\}$$
$$= \frac{1}{2}\{\dot{q}_2\}^T[M_3]\{\dot{q}_2\} \tag{4.23}$$

where $[M_3]$ is the mass matrix of element 3,

$$[M_3] = \int_0^{l_3}\rho_2[C_3]^T[C_3]dx \tag{4.24}$$

and $l_3$is the length of element 3.

By considering $X_3 = 0$ for element 3, the submatrices of $[M_3]$ can be derived as

$$M_3(1,1) = \rho_2\begin{bmatrix} l_3 & 0 \\ 0 & l_3 \end{bmatrix} \tag{4.25}$$

$M_3(1,2)$ is the coupling term between translation and rotation,

$$M_3(1,2) = \rho_2 l_3\begin{Bmatrix} \frac{1}{2}(l_3+u_5)\sin\alpha_2 - \frac{1}{144}l_3(\theta_4-\theta_5)^2\cos\alpha_2 \\ \frac{1}{2}(l_3+u_5)\cos\alpha_2 - \frac{1}{12}l_3(\theta_4-\theta_5)\sin\alpha_2 \end{Bmatrix} \tag{4.26}$$

with a size of 2 by 1.

$M_3(1,3)$ is the coupling term between translation and deformation,

$$M_3(1,3) = \frac{1}{2}\rho_2 l_3\begin{bmatrix} -\frac{1}{6}l_3\sin\alpha_2 & \cos\alpha_2 & 0 \\ \frac{1}{6}l_3\cos\alpha_2 & \sin\alpha_2 & 0 \end{bmatrix} \tag{4.27}$$

with size 2 by 3.

$$M_3(2,2) = \frac{1}{210}l_3\rho_2\left(70l_3^2 + 2\theta_4^2l_3^2 - 3l_3^2\theta_4\theta_5 + 140l_3u_5 + 70u_5^2 + 2\theta_5^2l_3^2\right) \tag{4.28}$$

$M_3(2,3)$ is the coupling term between rotation and deformation,

$$M_3(2,3) = \frac{1}{60}\rho_2 l_3^2\langle 2(l_3+u_5),\ -(2\theta_4-3\theta_5),\ 0\ \rangle \tag{4.29}$$

with size 1 by 3.

$$M_3(3,3) = \rho_2 l_3\begin{bmatrix} \frac{1}{105}l_3^2 & 0 & 0 \\ 0 & \frac{1}{3} & 0 \\ 0 & 0 & 0 \end{bmatrix} \tag{4.30}$$

with size 3 by 3.

By symmetry, the other components are

$$M_3(2,1) = M_3(1,2)^T \tag{4.31}$$

$$M_3(3,1) = M_3(1,3)^T \tag{4.32}$$

$$M_3(3,2) = M_3(2,3)^T \tag{4.33}$$

$[M_3]$ in totality is shown in Appendix A.

From the expressions of the components of the mass matrices of these elements, we can recognize that the mass matrix is a function of rigid coordinate α_i and elastic coordinates vector $\{e_i\}$. There exist couplings between rigid-body translation and rotation, couplings between rigid-body translation and elastic deformation, and couplings between rigid-body rotation and elastic deformation, all of which will contribute to the nonlinearity of the dynamic behavior of the system.

Recalling equations 4.6, 4.12, and 4.23, the kinetic energy of the system can be derived by summation as follows,

$$\begin{aligned} T &= \sum_{j=1}^{3} T_j \\ &= \frac{1}{2}\{\dot{q}_1\}^T([M_1] + [M_2])\{\dot{q}_1\} + \frac{1}{2}\{\dot{q}_2\}^T[M_3]\{\dot{q}_2\} \\ &= \frac{1}{2}\{\dot{q}\}^T[M]\{\dot{q}\} \end{aligned} \tag{4.34}$$

where $[M]$ is the mass matrix of the system with a size of 13 by 13,

$$[M] = \begin{bmatrix} M_1 + M_2 & 0 \\ 0 & M_3 \end{bmatrix} \tag{4.35}$$

and $\{\dot{q}\}$ is the generalized velocity vector of the system,

$$\{\dot{q}\} = \begin{pmatrix} \dot{\alpha}_1 \\ \dot{e}_1 \\ \underline{\dot{R}}_2 \\ \dot{\alpha}_2 \\ \dot{e}_2 \end{pmatrix} \tag{4.36}$$

4. 2 Potential energy of the system

For the system to work under the condition of zero gravity, the elastic strain energy of the components has to be the unique source of the potential energy of the system. According to Euler-Bernoulli beam theory with shear effect negligible, the potential energy for a uniform beam element j on body i can be expressed as

$$V_j = \frac{1}{2}\int_0^l E_i\left[I_i(v'')^2 + A_i(u')^2\right]dx \tag{4.37}$$

where the prime means differentiation with respect to spatial element coordinate x, E_i is the modulus of elasticity, I_i is the area moment of inertia and A_i is the cross-sectional area of body i.

From equation 3.16 we can arrive at

$$u = \langle 1 \quad 0 \rangle [N]\{d_j\} \tag{4.38}$$

$$v = \langle 0 \quad 1 \rangle [N]\{d_j\} \tag{4.39}$$

Differentiating both sides of equation 4.38 with respect to x leads to

$$u' = \langle 1 \quad 0 \rangle [N']\{d_j\} \tag{4.40}$$

Double differentiation of both sides of equation 4.39 with respect to x leads to

$$v'' = \langle 0 \quad 1 \rangle [N'']\{d_j\} \tag{4.41}$$

Substituting equation 4.40 and equation 4.41 into equation 4.37 leads to

$$\begin{aligned} V_j &= \frac{1}{2}\langle d_j \rangle \left(\int_0^l E_i I_i [N'']^T \begin{bmatrix} 0 & 0 \\ 0 & 1 \end{bmatrix} [N'']dx \right. \\ &\qquad \left. + \int_0^l E_i A_i [N']^T \begin{bmatrix} 1 & 0 \\ 0 & 0 \end{bmatrix} [N']\,dx \right) \{d_j\} \\ &= \frac{1}{2}\langle d_j \rangle [K_j^e]\{d_j\} \\ &= \frac{1}{2}\{e_i\}^T [K_j]\{e_i\} \end{aligned} \tag{4.42}$$

where $[K_j^e]$ is the stiffness matrix of element j.

and

$$[K_j^e] = \int_0^l E_i I_i [N'']^T \begin{bmatrix} 0 & 0 \\ 0 & 1 \end{bmatrix} [N''] dx + \int_0^l E_i A_i [N']^T \begin{bmatrix} 1 & 0 \\ 0 & 0 \end{bmatrix} [N'] dx$$

$$= \frac{E_i I_i}{l} \begin{bmatrix} \frac{A_i}{I_i} & 0 & 0 & -\frac{A_i}{I_i} & 0 & 0 \\ 0 & \frac{12}{l^2} & \frac{6}{l} & 0 & \frac{12}{l^2} & \frac{6}{l} \\ & & 4 & 0 & -\frac{6}{l} & 2 \\ & \text{symmetric} & & \frac{A_i}{I_i} & 0 & 0 \\ & & & & \frac{12}{l^2} & -\frac{6}{l} \\ & & & & & 4 \end{bmatrix} \tag{4.43}$$

and $[K_j]$ is the stiffness matrix of element j expressed in the body-fixed moving frame,

$$[K_j] = [B_j]^T [K_j^e] [B_j] \tag{4.44}$$

$[K_j]$ can be explicitly expressed as follows:

For element 1,

$$[K_1] = [B_1]^T [K_1^e] [B_1]$$

$$= \frac{E_1 I_1}{l_1} \begin{bmatrix} 4 & 0 & 2 & 0 & 0 & 0 \\ 0 & \frac{A_1}{I_1} & 0 & 0 & 0 & 0 \\ 2 & 0 & 4 & 0 & 0 & 0 \\ 0 & 0 & 0 & 0 & 0 & 0 \\ 0 & 0 & 0 & 0 & 0 & 0 \\ 0 & 0 & 0 & 0 & 0 & 0 \end{bmatrix} \tag{4.45}$$

For element 2,

$$[K_2] = \frac{E_1 I_1}{l_2} \begin{bmatrix} 0 & 0 & 0 & 0 & 0 & 0 \\ 0 & \frac{A_1}{I_1} & 0 & -\frac{A_1}{I_1} & 0 & 0 \\ 0 & 0 & 4 & 0 & -\frac{6}{l_2} & 2 \\ 0 & -\frac{A_1}{I_1} & 0 & \frac{A_1}{I_1} & 0 & 0 \\ 0 & 0 & -\frac{6}{l_2} & 0 & \frac{12}{l_2^2} & -\frac{6}{l_2} \\ 0 & 0 & 2 & 0 & -\frac{6}{l_2} & 4 \end{bmatrix} \tag{4.46}$$

Similarly, for element 3

$$[K_3] = \frac{E_2 I_2}{l_3} \begin{bmatrix} 4 & 0 & 0 \\ 0 & \frac{A_2}{I_2} & 0 \\ 0 & 0 & 0 \end{bmatrix} \tag{4.47}$$

The potential energy for body i is the summation as

$$\begin{aligned} V &= \sum_{j=1}^{3} V_j \\ &= \frac{1}{2}\{e_1\}^T([K_1]+[K_2])\{e_1\} + \frac{1}{2}\{e_2\}^T[K_3]\{e_2\} \\ &= \frac{1}{2}\{q\}^T[K]\{q\} \end{aligned} \tag{4.48}$$

where $[K]$ is the stiffness matrix of the system,

$$[K] = \begin{bmatrix} 0 & 0 & 0 & 0 & 0 & 0 \\ 0 & [K_1]+[K_2] & 0 & 0 & 0 & 0 \\ 0 & 0 & 0 & 0 & 0 & 0 \\ 0 & 0 & 0 & 0 & 0 & 0 \\ 0 & 0 & 0 & 0 & 0 & 0 \\ 0 & 0 & 0 & 0 & 0 & [K_3] \end{bmatrix} \tag{4.49}$$

Considering equations 4.45 and 4.46, we can find

$$[K_1]+[K_2] = \frac{E_1 I_1}{l_1 l_2} \begin{bmatrix} 4l_2 & 0 & 2l_2 & 0 & 0 & 0 \\ 0 & \frac{A_1(l_1+l_2)}{I_1} & 0 & -\frac{A_1 l_1}{I_1} & 0 & 0 \\ 2l_2 & 0 & 4(l_1+l_2) & 0 & -\frac{6l_1}{l_2} & 2l_1 \\ 0 & -\frac{A_1 l_1}{I_1} & 0 & \frac{A_1 l_1}{I_1} & 0 & 0 \\ 0 & 0 & -\frac{6l_1}{l_2} & 0 & \frac{12l_1}{l_2^2} & -\frac{6l_1}{l_2} \\ 0 & 0 & 2l_1 & 0 & -\frac{6l_1}{l_2} & 4l_1 \end{bmatrix} \tag{4.50}$$

4. 3 Constraint equations and Jacobian matrix

The motion of the components of the system that are the leaf and link is constrained by joint points $O(O')$, O'' and the prescribed trajectory (point H moving along Y-axis), as shown in Figure 3.4. So certain constraint conditions have to be satisfied and always hold from the start to the end of the motion if the system is to function properly. As shown in the following subsections, all the constraints are

holonomic and the formulation of constrained generalized coordinates is adopted because it has an apparent advantage of calculating the constrained generalized forces in addition to the key motion parameters concerned. That is also why the constraint Jacobian is introduced. In the following subsections the constraint conditions in three cases are discussed based on the 3-element model.

4. 3. 1 Case 1: In the process of deployment

In this subsection we will analyze the related constraints in the process of deployment from the start, but before full deployment is reached.

In Chapter 3, the constraints at the joint $O(O')$ have already been taken into account when formulating the generalized coordinates $\{q\}$, so it is not necessary to consider them again.

At joint O'', node 2 on the leaf is coincided with node 4 on the link, i.e.

$$\underline{r}_{11}\Big|_{x=l_1} = \underline{r}_{23}\Big|_{x=0} \tag{4.51}$$

where l_1 is length of section $O'O''$ on the leaf.

Substituting equations 3.22 and 3.24 into the upper expression, we get

$$\begin{bmatrix} \cos\alpha_1 & -\sin\alpha_1 \\ \sin\alpha_1 & \cos\alpha_1 \end{bmatrix} \begin{Bmatrix} l_1 + u_2 \\ 0 \end{Bmatrix} = \begin{Bmatrix} R_2^x \\ R_2^y \end{Bmatrix} \tag{4.52}$$

which forms the following two constraint equations

$$\Phi_1 = (l_1 + u_2)\cos\alpha_1 - R_2^x = 0 \tag{4.53}$$

$$\Phi_2 = (l_1 + u_2)\sin\alpha_1 - R_2^y = 0 \tag{4.54}$$

Recalling equation 3.17, the position of joint H is

$$\begin{aligned} \underline{r}_H &= \underline{r}_{23}\Big|_{x=l_3} \\ &= \begin{Bmatrix} R_2^x \\ R_2^y \end{Bmatrix} + [A_2]\left(\begin{Bmatrix} l_3 \\ 0 \end{Bmatrix} + [N]\Big|_{x=l_3}[B_3]\{e_2\}\right) \\ &= \begin{Bmatrix} R_2^x \\ R_2^y \end{Bmatrix} + [A_2]\begin{Bmatrix} l_3 + u_5 \\ 0 \end{Bmatrix} \end{aligned} \tag{4.55}$$

where the transformation matrix

$$[A_2]=\begin{bmatrix} \cos\alpha_2 & -\sin\alpha_2 \\ \sin\alpha_2 & \cos\alpha_2 \end{bmatrix} \tag{4.56}$$

In simplified component form

$$r_H^x = R_2^x + (l_3 + u_5)\cos\alpha_2 \tag{4.57}$$

$$r_H^y = R_2^y + (l_3 + u_5)\sin\alpha_2 \tag{4.58}$$

where l_3 is the length of $O''H$ on the link.

Because joint H is restricted to move on the Y-axis, the component r_H^x on the X-axis should always be zero, and this leads to the third constraint condition,

$$\Phi_3 = R_2^x + (l_3 + u_5)\cos\alpha_2 = 0 \tag{4.59}$$

The totality of the constraints is named

$$\left\{C_1(\{q\})\right\} = \begin{Bmatrix} \Phi_1 \\ \Phi_2 \\ \Phi_3 \end{Bmatrix} = \{0\} \tag{4.60}$$

which is a function of generalized coordinates.

In the case of the 3-element model, the vector of generalized coordinates is repeated here,

$$\{q\} = \langle \alpha_1 \;\; \theta_1 \;\; u_2 \;\; \theta_2 \;\; u_3 \;\; v_3 \;\; \theta_3 \;\; R_2^x \;\; R_2^y \;\; \alpha_2 \;\; \theta_4 \;\; u_5 \;\; \theta_5 \rangle^T$$

Now we can derive the constraint conditions at velocity level by differentiation with respect to time t,

$$\frac{\partial\left\{C_1(\{q\})\right\}}{\partial\{q\}}\{\dot{q}\} = \{0\} \quad \text{or}$$

$$[J_1]\{\dot{q}\} = \{0\} \tag{4.61}$$

where $[J_1]$ is the constraint Jacobian matrix, which is detailed in Appendix A.

By differentiating both sides of equation 4.61 with respect to time t we can arrive at the constraint conditions at acceleration level

$$[\dot{J}_1]\{\dot{q}\} + [J_1]\{\ddot{q}\} = \{0\} \text{ or}$$

$$[J_1]\{\ddot{q}\} = -[\dot{J}_1]\{\dot{q}\} \tag{4.62}$$

where double dots mean the second-order differentiation with respect to time t, and the time derivative of the constraint Jacobian matrix is also shown in Appendix A.

Equation 4.62 will be combined with equations of motion of the system to form differential-algebraic equations for the system to analyze the dynamic response in the process of deployment.

4. 3. 2 Case 2: an additional constraint at full deployment

When the system reaches the full deployment shown in Figure 4.1, the joint H moves to point S and is fixed at that point hence forward. The distance between point O and S is assigned as l_4. So an extra constraint condition is added to those of Case 1.

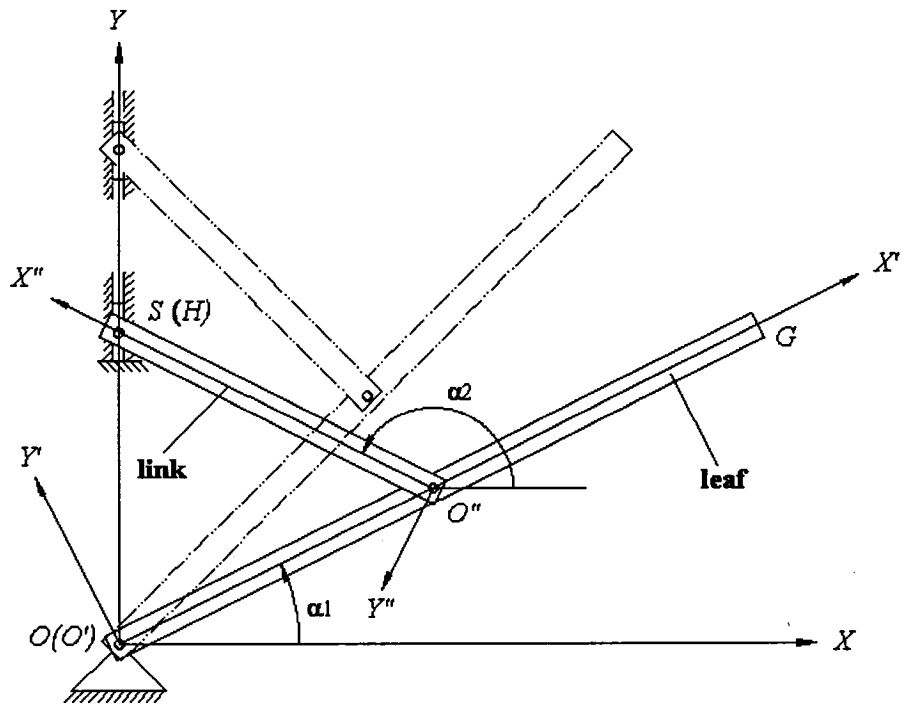

Figure 4.1 The position of full deployment

Considering equation 4.58, we get the fourth constraint

$$\Phi_4 = R_2^y + (l_3 + u_5)\sin\alpha_2 - l_4 = 0 \tag{4.63}$$

The totality of the constraints then becomes

$$\left\{C_2(\{q\})\right\} = \langle \Phi_1 \quad \Phi_2 \quad \Phi_3 \quad \Phi_4 \rangle^T = \{0\} \tag{4.64}$$

Similarly we can derive the constraint conditions at velocity level by differentiation with respect to time t,

$$\frac{\partial\{C_2(\{q\})\}}{\partial\{q\}}\{\dot{q}\} = \{0\} \quad \text{or}$$

$$[J_2]\{\dot{q}\} = \{0\} \tag{4.65}$$

where $[J_2]$ is the constraint Jacobian matrix, which is detailed in Appendix A.

By differentiating both sides of equation 4.65 with respect to time t we can arrive at the constraint conditions at acceleration level

$$[\dot{J}_2]\{\dot{q}\} + [J_2]\{\ddot{q}\} = \{0\} \quad \text{or}$$

$$[J_2]\{\ddot{q}\} = -[\dot{J}_2]\{\dot{q}\} \tag{4.66}$$

where double dots mean the second-order differentiation with respect to time t, and the time derivative of the constraint Jacobian matrix is also shown in Appendix A.

Equation 4.66 will be combined with equations of motion of the system to form differential-algebraic equations for the system in analyzing the vibration at the full deployment.

4. 3. 3 Case 3: Pure rigid-body mode with elastic deformation constrained

As a totally different situation comparing to Case 1 and Case 2, we can take into account only the rigid-body motion with the deformation of the components neglected, from which we can conclude that all of the elastic generalized coordinates are constrained.

For the leaf the additional constraints are

$$\{\Phi_5\} = \{e_1\} = \{0\} \tag{4.67}$$

For the link

$$\{\Phi_6\} = \{e_2\} = \{0\} \tag{4.68}$$

From equation 3.10 and equation 3.13 we know for the 3-element model the additional constraints are

$$\{\Phi_5\} = \langle\ \theta_1 \quad u_2 \quad \theta_2 \quad u_3 \quad v_3 \quad \theta_3 \rangle^T = \{0\} \tag{4.69}$$

and

$$\{\Phi_6\} = \langle\ \theta_4 \quad u_5 \quad \theta_5\ \rangle^T = \{0\} \tag{4.70}$$

Because in this case only the rigid-body mode is considered, the generalized velocities $\{\dot{q}\}$ should vanish once joint H moves to point S and stays there when the system is assumed to be stationary. So we do not need to consider the constraint Φ_4 proposed in Case 2.

Then the totality of the constraints becomes

$$\left\{C_3(\{q\})\right\} = \langle \Phi_1 \quad \Phi_2 \quad \Phi_3 \quad \Phi_5^T \quad \Phi_6^T \rangle^T = \{0\} \tag{4.71}$$

In the same way we can derive the constraint conditions at velocity level by differentiation with respect to time t,

$$\frac{\partial\left\{C_3(\{q\})\right\}}{\partial\{q\}}\{\dot{q}\} = \{0\} \quad \text{or}$$

$$[J_3]\{\dot{q}\} = \{0\} \tag{4.72}$$

where $[J_3]$ is the constraint Jacobian matrix, which is detailed in Appendix A.

By differentiating both sides of equation 4.72 with respect to time t, we can derive the constraint conditions at acceleration level

$$[\dot{J}_3]\{\dot{q}\} + [J_3]\{\ddot{q}\} = \{0\} \quad \text{or}$$

$$[J_3]\{\ddot{q}\} = -[\dot{J}_3]\{\dot{q}\} \tag{4.73}$$

The time derivative of the constraint Jacobian matrix is also shown in Appendix A.

Equation 4.73 will be used to form differential-algebraic equations in analyzing the rigid-body motion.

4. 4 Generalized forces

The generalized forces corresponding to the generalized coordinates can be derived by formulating the virtual work done by the external forces.

In this model we assume the force

$$\underline{F}=\begin{Bmatrix} 0 \\ -F_H \end{Bmatrix} \tag{4.74}$$

acting at point H and $F_H \geq 0$.

Recalling equation 4.57, we get the following variation of $\underline{r}_H$

$$\delta \underline{r}_H = \begin{Bmatrix} \delta R_2^x \\ \delta R_2^y \end{Bmatrix} + [A_2'] \begin{Bmatrix} l_3 + u_5 \\ 0 \end{Bmatrix} \delta\alpha_2 + [A_2] \begin{Bmatrix} \delta u_5 \\ 0 \end{Bmatrix} \tag{4.75}$$

where the prime means differentiation with respect to spatial coordinate α_2.

The virtual work of the nonconservative force is

$$\begin{aligned} \delta W^{appl.nc} &= \underline{F} \cdot \delta \underline{r}_H \\ &= -F_H \delta R_2^y - F_H (l_3 + u_5)\cos\alpha_2 \delta\alpha_2 - F_H \sin\alpha_2 \delta u_5 \\ &= \begin{bmatrix} -F_H & -F_H(l_3+u_5)\cos\alpha_2 & -F_H\sin\alpha_2 \end{bmatrix} \begin{Bmatrix} \delta R_2^y \\ \delta\alpha_2 \\ \delta u_5 \end{Bmatrix} \\ &= \langle \bar{Q} \rangle \begin{Bmatrix} \delta R_2^y \\ \delta\alpha_2 \\ \delta u_5 \end{Bmatrix} \end{aligned} \tag{4.76}$$

where

$$\langle \bar{Q} \rangle = \langle -F_H \quad -F_H(l_3+u_5)\cos\alpha_2 \quad -F_H\sin\alpha_2 \rangle \tag{4.77}$$

$$\begin{Bmatrix} \delta R_2^y \\ \delta\alpha_2 \\ \delta u_5 \end{Bmatrix} = [B_v]\delta\{q\} \tag{4.78}$$

in which $[B_v]$ is the transformation matrix,

$$[B_v] = \begin{bmatrix} 0 & 0 & 0 & 0 & 0 & 0 & 0 & 0 & 1 & 0 & 0 & 0 & 0 \\ 0 & 0 & 0 & 0 & 0 & 0 & 0 & 0 & 0 & 1 & 0 & 0 & 0 \\ 0 & 0 & 0 & 0 & 0 & 0 & 0 & 0 & 0 & 0 & 0 & 1 & 0 \end{bmatrix} \tag{4.79}$$

Substituting equation 4.83 into equation 4.81 leads to

$$\delta W^{appl.nc} = \langle \bar{Q} \rangle [B_v] \delta\{q\} \tag{4.80}$$

So the generalized forces are

$$\{Q^{appl.nc}\} = (\langle \bar{Q} \rangle [B_v])^T$$
$$= [B_v]^T \langle \bar{Q} \rangle^T$$

$$= \begin{pmatrix} 0 \\ 0 \\ 0 \\ 0 \\ 0 \\ 0 \\ 0 \\ 0 \\ -F_H \\ -F_H(l_3 + u_5)\cos\alpha_2 \\ 0 \\ -F_H \sin\alpha_2 \\ 0 \end{pmatrix} \tag{4.81}$$

4. 5 Governing equations of motion for the system

At first, we derive the equations of motion for the process of deployment of the system, which corresponds to Case 1, the constraint conditions described in Section 4. 3.1.

Once the kinetic and potential energy, the generalized nonconservative forces and the constraint Jacobian for the system have been found, the governing equations of motion of the system are then developed by invoking Lagrangian equations with multipliers,

$$\frac{\partial}{\partial t}\left(\frac{\partial L}{\partial \{\dot{q}\}}\right)^T - \left(\frac{\partial L}{\partial \{q\}}\right)^T = \{Q^{appl.nc}\} + [J_1]^T \{\lambda\} \tag{4.82}$$

where Lagrangian

$$L = T - V \tag{4.83}$$

and $\{\lambda\}$ is the vector of Lagrangian multipliers.

Considering equation 4.34 and equation 4.48 the Lagrangian becomes

$$L = \frac{1}{2}\{\dot{q}\}^T[M]\{\dot{q}\} - \frac{1}{2}\{q\}^T[K]\{q\}$$

then

$$\left(\frac{\partial L}{\partial\{\dot{q}\}}\right)^T = [M]\{\dot{q}\} \qquad \frac{\partial}{\partial t}\left(\frac{\partial L}{\partial\{\dot{q}\}}\right)^T = [M]\{\ddot{q}\} + [\dot{M}]\{\dot{q}\}$$

$$\left(\frac{\partial L}{\partial\{q\}}\right)^T = -[K]\{q\} + \left(\frac{\partial T}{\partial\{q\}}\right)^T$$

Substituting these terms into equation 4.82 yields the following equations of motion for the system

$$[M]\{\ddot{q}\} + [K]\{q\} = -[\dot{M}]\{\dot{q}\} + \left(\frac{\partial T}{\partial\{q\}}\right)^T + \{Q^{appl.nc}\} + [J_1]^T\{\lambda\} \tag{4.84}$$

where

$$[\dot{M}] = \begin{bmatrix} \dot{M}_1 + \dot{M}_2 & 0 \\ 0 & \dot{M}_3 \end{bmatrix} \tag{4.85}$$

and

$$\left(\frac{\partial T}{\partial\{q\}}\right)^T = \begin{pmatrix} \left(\frac{\partial T_1}{\partial\{q_1\}}\right)^T + \left(\frac{\partial T_2}{\partial\{q_1\}}\right)^T \\ \left(\frac{\partial T_3}{\partial\{q_2\}}\right)^T \end{pmatrix} \tag{4.86}$$

As previously indicated, the constraint conditions always have to be met. Combining equation 4.84 with equation 4.62, we finally get the differential-algebraic equations for system

$$\begin{bmatrix} M & -J_1^T \\ J_1 & 0 \end{bmatrix}\begin{Bmatrix} \ddot{q} \\ \lambda \end{Bmatrix} = \begin{Bmatrix} -[K]\{q\} - [\dot{M}]\{\dot{q}\} + \left(\frac{\partial T}{\partial\{q\}}\right)^T + \{Q^{appl.nc}\} \\ -[\dot{J}_1]\{\dot{q}\} \end{Bmatrix} \tag{4.87}$$

which possess 16 unknowns.

The following is to find $[\dot{M}]$, the time derivative of mass matrix, and the spatial derivative of the kinetic energy of the system $\left(\frac{\partial T}{\partial \{q\}}\right)^T$.

Referring equation 4.35 leads to

$$[\dot{M}] = \begin{bmatrix} \dot{M}_1 + \dot{M}_2 & 0 \\ 0 & \dot{M}_3 \end{bmatrix} \tag{4.88}$$

Recalling equations 4.7 to 4.11, we can compute the components of $[\dot{M}_1]$,

$$\begin{aligned} \dot{M}_1(1,1) = \rho_1 l_1 \Big(& \frac{2}{3} l_1 \dot{u}_2 + \frac{2}{105} l_1^2 \theta_{_1} \dot{\theta}_{_1} - \frac{1}{70} l_1^2 \dot{\theta}_{_1} \theta_{_2} \\ & - \frac{1}{70} l_1^2 \theta_{_1} \dot{\theta}_{_2} + \frac{2}{3} u_2 \dot{u}_2 + \frac{2}{105} l_1^2 \theta_{_2} \dot{\theta}_{_2} \Big) \end{aligned} \tag{4.89}$$

$$\dot{M}_1(1,2) = \rho_1 l_1^2 \Big\langle \frac{1}{30} \dot{u}_2 \quad -\frac{1}{30} \dot{\theta}_{_1} + \frac{1}{20} \dot{\theta}_{_2} \quad -\frac{1}{20} \dot{u}_2 \quad 0 \quad 0 \quad 0 \Big\rangle \tag{4.90}$$

with size 1 by 6.

$$\dot{M}_1(2,2) = [0] \tag{4.91}$$

with size 6 by 6.

By symmetry,

$$\dot{M}_1(2,1) = \dot{M}_1(1,2)^T = \rho_1 l_1^2 \begin{pmatrix} \frac{1}{30} \dot{u}_2 \\ -\frac{1}{30} \dot{\theta}_{_1} + \frac{1}{20} \dot{\theta}_{_2} \\ -\frac{1}{20} \dot{u}_2 \\ 0 \\ 0 \\ 0 \end{pmatrix} \tag{4.92}$$

Similarly, $[\dot{M}_2]$ can be partitioned as

$$\begin{aligned} \dot{M}_2(1,1) = & \\ & \rho_1 l_2 \Big(l_1 \dot{u}_2 + \frac{1}{3} l_2 \dot{u}_2 + l_1 \dot{u}_3 + \frac{2}{3} l_2 \dot{u}_3 + \frac{2}{3} u_2 \dot{u}_2 + \frac{1}{3} \dot{u}_2 u_3 + \frac{1}{3} u_2 \dot{u}_3 \\ & + \frac{2}{105} l_2^2 \theta_2 \dot{\theta}_2 + \frac{13}{210} l_2 \dot{\theta}_2 v_3 + \frac{13}{210} l_2 \theta_2 \dot{v}_3 - \frac{1}{70} l_2^2 \dot{\theta}_2 \theta_3 - \frac{1}{70} l_2^2 \theta_2 \dot{\theta}_3 \\ & + \frac{2}{3} u_3 \dot{u}_3 + \frac{26}{35} v_3 \dot{v}_3 - \frac{11}{105} l_2 \dot{v}_3 \theta_3 - \frac{11}{105} l_2 v_3 \dot{\theta}_3 + \frac{2}{105} l_2^2 \theta_3 \dot{\theta}_3 \Big) \end{aligned} \tag{4.93}$$

$$\dot{M}_2(1,2) =$$
$$\rho_1 l_2 \langle 0, -\frac{1}{60}(3l_2\dot{\theta}_2 + 9\dot{v}_3 - 2l_2\dot{\theta}_3), \frac{1}{60}l_2(3\dot{u}_2 + 2\dot{u}_3),$$
$$-\frac{1}{60}(2l_2\dot{\theta}_2 + 21\dot{v}_3 - 3l_2\dot{\theta}_3), \frac{1}{20}(3\dot{u}_2 + 7\dot{u}_3), -\frac{1}{60}l_2(2\dot{u}_2 + 3\dot{u}_3\rangle \quad (4.94)$$

with size 1 by 6.

$$\dot{M}_2(2,2) = [0] \quad (4.95)$$

with size 6 by 6.

By symmetry,

$$\dot{M}_2(2,1) = \dot{M}_2(1,2)^T = \rho_1 l_2 \begin{pmatrix} 0 \\ -\frac{1}{60}(3l_2\dot{\theta}_2 + 9\dot{v}_3 - 2l_2\dot{\theta}_3) \\ \frac{1}{60}l_2(3\dot{u}_2 + 2\dot{u}_3) \\ -\frac{1}{60}(2l_2\dot{\theta}_2 + 21\dot{v}_3 - 3l_2\dot{\theta}_3) \\ \frac{1}{20}(3\dot{u}_2 + 7\dot{u}_3) \\ -\frac{1}{60}l_2(2\dot{u}_2 + 3\dot{u}_3 \end{pmatrix} \quad (4.96)$$

For element 3, we have

$$\dot{M}_3(1,1) = \begin{bmatrix} 0 & 0 \\ 0 & 0 \end{bmatrix} \quad (4.97)$$

$$\dot{M}_3(1,2) = \rho_2 l_3 \left\{ \begin{array}{l} \frac{1}{2}(l_3 + u_5)\cos\alpha_2\dot{\alpha}_2 + \frac{1}{2}\dot{u}_5\sin\alpha_2 \\ -\frac{1}{2}(l_3 + u_5)\sin\alpha_2\dot{\alpha}_2 + \frac{1}{2}\dot{u}_5\cos\alpha_2 \\ \quad + \frac{1}{144}l_3(\theta_4 - \theta_5)^2\sin\alpha_2\dot{\alpha}_2 - \frac{1}{72}l_3(\theta_4 - \theta_5)(\dot{\theta}_4 - \dot{\theta}_5)\cos\alpha_2 \\ \quad - \frac{1}{12}l_3(\theta_4 - \theta_5)\cos\alpha_2\dot{\alpha}_2 - \frac{1}{12}l_3(\dot{\theta}_4 - \dot{\theta}_5)\sin\alpha_2 \end{array} \right\} \quad (4.98)$$

with a size of 2 by 1.

$$\dot{M}_3(1,3) = \frac{1}{2}\rho_2 l_3 \begin{bmatrix} -\frac{1}{6}l_3\cos\alpha_2\dot{\alpha}_2 & -\sin\alpha_2\dot{\alpha}_2 & 0 \\ -\frac{1}{6}l_3\sin\alpha_2\dot{\alpha}_2 & \cos\alpha_2\dot{\alpha}_2 & 0 \end{bmatrix} \quad (4.99)$$

with size 2 by 3.

$$\dot{M}_3(2,2) = \frac{1}{210}l_3\rho_2 \left(4l_3^2\theta_4\dot{\theta}_4 - 3l_3^2\dot{\theta}_4\theta_5 - 3l_3^2\theta_4\dot{\theta}_5 + 140l_3\dot{u}_5 + 140u_5\dot{u}_5 + 4l_3^2\theta_5\dot{\theta}_5\right) \quad (4.100)$$

$$\dot{M}_3(2,3) = \frac{1}{60}\rho_2 l_3^2 \langle 2\dot{u}_5 \quad -(2\dot{\theta}_4 - 3\dot{\theta}_5) \quad 0 \rangle \quad (4.101)$$

with size 1 by 3.

$$\dot{M}_3(3,3) = [0] \tag{4.102}$$

with size 3 by 3.

By symmetry, the other components are

$$\dot{M}_3(2,1) = \dot{M}_3(1,2)^T \tag{4.103}$$

$$\dot{M}_3(3,1) = \dot{M}_3(1,3)^T \tag{4.104}$$

$$\dot{M}_3(3,2) = \dot{M}_3(2,3)^T \tag{4.105}$$

Then, the spatial derivatives of the kinetic energy can be expressed as

$$\left(\frac{\partial T_1}{\partial\{q_1\}}\right)^T = \begin{Bmatrix} \dfrac{\partial T_1}{\partial \alpha_1} \\ \left(\dfrac{\partial T_1}{\partial\{e_1\}}\right)^T \end{Bmatrix} \tag{4.106}$$

in which

$$\frac{\partial \mathrm{T}_1}{\partial \alpha_1} = \frac{1}{2}\{\dot{q}_1\}^T \frac{\partial [M_1]}{\partial \alpha_1} \{\dot{q}_1\} = 0 \tag{4.107}$$

Because

$$\frac{\partial [M_1]}{\partial \alpha_1} = [0] \tag{4.108}$$

with a size of 7 by 7.

The following is about $\left(\dfrac{\partial T_1}{\partial\{e_1\}}\right)^T$ the spatial derivatives of kinetic energy with respect to elastic coordinates $\{e_1\}$:

$$\left(\frac{\partial T_1}{\partial\{e_1\}}\right)^T = \left\langle \frac{\partial T_1}{\partial \theta_1} \quad \frac{\partial T_1}{\partial u_2} \quad \frac{\partial T_1}{\partial \theta_2} \quad \frac{\partial T_1}{\partial u_3} \quad \frac{\partial T_1}{\partial v_3} \quad \frac{\partial T_1}{\partial \theta_3} \right\rangle^T \tag{4.109}$$

where

$$\frac{\partial T_1}{\partial \theta_1} = \frac{1}{2}\{\dot{q}_1\}^T \frac{\partial [M1]}{\partial \theta_1} \{\dot{q}_1\} \tag{4.110}$$

in which

$$\frac{\partial [M1]}{\partial \theta_1}(1,1) = \rho_1 l_1 \left(\frac{2}{105} l_1^2 \theta_1 - \frac{1}{70} l_1^2 \theta_2\right) \tag{4.111}$$

$$\frac{\partial [M1]}{\partial \theta_1}(1,2) = \rho_1 l_1^2 \left\langle 0 \quad -\frac{1}{30} \quad 0 \quad 0 \quad 0 \quad 0 \right\rangle \tag{4.112}$$

and

$$\frac{\partial[M1]}{\partial \theta_1}(2,2) = [0] \tag{4.113}$$

with size 6 by 6.

By symmetry,

$$\frac{\partial[M1]}{\partial \theta_1}(2,1) = \left(\frac{\partial[M1]}{\partial \theta_1}(1,2)\right)^T = \rho_1 l_1^2 \begin{pmatrix} 0 \\ -\frac{1}{30} \\ 0 \\ 0 \\ 0 \\ 0 \end{pmatrix} \tag{4.114}$$

Substituting equations 4.111 to 4.114 into equation 4.110 leads to

$$\frac{\partial T_1}{\partial \theta_1} = \frac{1}{2}\rho_1 l_1 \dot{\alpha}_1^2 \left(\frac{2}{105} l_1^2 \theta_1 - \frac{1}{70} l_1^2 \theta_2\right) - \frac{1}{30}\rho_1 \dot{\alpha}_1 l^2 \dot{u}_2 \tag{4.115}$$

By following the same way, the other 5 components of $\left(\frac{\partial T_1}{\partial \{e_1\}}\right)^T$ can be calculated, and further repetition of the process derives

$$\left(\frac{\partial T_2}{\partial \{q_1\}}\right)^T = \begin{Bmatrix} \frac{\partial T_2}{\partial \alpha_1} \\ \left(\frac{\partial T_1}{\partial \{e_1\}}\right)^T \end{Bmatrix} \tag{4.116}$$

and

$$\left(\frac{\partial T_3}{\partial \{q_2\}}\right)^T = \begin{pmatrix} \left(\frac{\partial T_3}{\partial \underline{R}_2}\right)^T \\ \frac{\partial T_3}{\partial \alpha_2} \\ \left(\frac{\partial T_i}{\partial \{e_2\}}\right)^T \end{pmatrix} \tag{4.117}$$

Now let us consider the equations of motion satisfying the constraint condition in Case 2 and Case 3. By referring to the aforementioned general process of derivation, we only need to exchange the constraint Jacobian of equation 4.87 for that of each case.

For Case 2 where the system arrives at full deployment we have

$$\begin{bmatrix} M & -J_2^T \\ J_2 & 0 \end{bmatrix} \begin{Bmatrix} \ddot{q} \\ \lambda \end{Bmatrix} = \begin{Bmatrix} -[K]\{q\} - [\dot{M}]\{\dot{q}\} + \left(\frac{\partial T}{\partial \{q\}}\right)^T + \{Q^{appl.nc}\} \\ -[\dot{J}_2]\{\dot{q}\} \end{Bmatrix} \tag{4.118}$$

by which we can analyze the induced vibration of deformation for the components. The equations involve 17 unknowns.

Now we have developed the necessary two sets of governing equations to simulate the opening process of the system from start to the full deployment.

For Case 3, the pure rigid-body mode, we obtain

$$\begin{bmatrix} M & -J_3^T \\ J_3 & 0 \end{bmatrix} \begin{Bmatrix} \ddot{q} \\ \lambda \end{Bmatrix} = \begin{Bmatrix} -[K]\{q\} - [\dot{M}]\{\dot{q}\} + \left(\frac{\partial T}{\partial \{q\}}\right)^T + \{Q^{appl.nc}\} \\ -[\dot{J}_3]\{\dot{q}\} \end{Bmatrix} \tag{4.119}$$

from which we can calculate the related dynamic parameters of rigid-body motion. The equations include 25 unknown parameters.

4. 6 Derivation of governing equations of motion by rigid-body dynamics

Next we develop the close-form governing equations of motion for the rigid-body mode following the formulation of constrained Lagrangian dynamics. As will be seen later, these equations also display high nonlinearity and can only be solved numerically.

Referring to Figure 4.2 we adopt α_1 and α_2 as the constrained generalized coordinates for the system in which only the inertial frame XOY is necessary. Then the kinetic energy of the system can be derived as

$$T = \frac{1}{2}\left(I'_1 + m_2 l_1^2\right)\dot{\alpha}_1{}^2 + \frac{1}{2} I'_2 \dot{\alpha}_2{}^2 + \frac{3}{2}\frac{l_1}{l_3} I'_2 \dot{\alpha}_1 \dot{\alpha}_2 \cos(\alpha_1 - \alpha_2) \tag{4.120}$$

where I_1' is the mass moment of inertia of the leaf about joint O, I_2' is the mass moment of inertia of the link about joint O'' and m_2 is the mass of the link.

Because we are considering the system without deformation and gravity, there exists no potential energy, so the Lagrangian

$$L = T \tag{4.121}$$

Applying the same force condition as equation 4.70, we obtain the following virtual work done by generalized nonconservative force

$$\delta W^{appl.nc} = -F_H l_1 \cos\alpha_1 \delta\alpha_1 - F_H l_3 \cos\alpha_2 \delta\alpha_2 \tag{4.122}$$

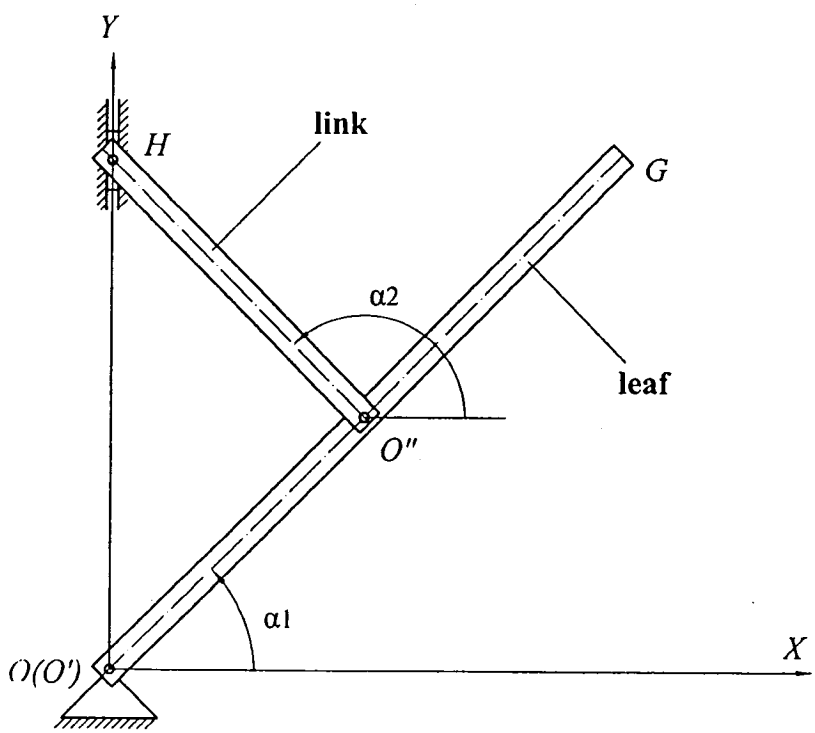

Figure 4.2 Configuration of rigid-body system

Considering the trajectory followed by the joint H, we have the following constraint equation

$$\Phi = l_1 \cos\alpha_1 + l_3 \cos\alpha_2 = 0 \tag{4.123}$$

The constraint Jacobian is

$$\langle J \rangle = \langle -l_1 \sin\alpha_1 \quad -l_3 \sin\alpha_2 \rangle \tag{4.124}$$

Invoking the Lagrangian equation and considering the constraint condition, we obtain

$$\begin{bmatrix} I_1' + m_2 l_1^2 & \frac{3}{2}\frac{l_1}{l_3} I_2' \cos(\alpha_1 - \alpha_2) & l_1 \sin\alpha_1 \\ \frac{3}{2}\frac{l_1}{l_3} I_2' \cos(\alpha_1 - \alpha_2) & I_2' \left(\frac{l_2}{l_3}\right)^3 & l_3 \sin\alpha_2 \\ -l_1 \sin\alpha_1 & -l_3 \sin\alpha_2 & 0 \end{bmatrix} \begin{pmatrix} \ddot{\alpha}_1 \\ \ddot{\alpha}_2 \\ \lambda \end{pmatrix} =$$

$$\begin{pmatrix} -\frac{3}{2}\frac{l_1}{l_3} I_2' \dot{\alpha}_2^2 \sin(\alpha_1 - \alpha_2) - F_H l_1 \cos\alpha_1 \\ \frac{3}{2}\frac{l_1}{l_3} I_2' \dot{\alpha}_1^2 \sin(\alpha_1 - \alpha_2) - F_H l_3 \cos\alpha 2 \\ l_1 \dot{\alpha}_1^2 \cos\alpha_1 + l_3 \dot{\alpha}_2^2 \cos\alpha_2 \end{pmatrix} \tag{4.125}$$

where l_2 is the distance between joint O'' and end point G on the leaf.

Equation 4.125 can be solved in the same way as equation 4.87.

Chapter 5

Solution of Equations of Motion of the System

5. 1 Solution of the differential-algebraic equations

As we can see from the previous section, the equations of motion for the system are a combination of differential and algebraic equations. The generalized coordinates included in vector $\{q\}$ and Lagrangian multipliers of vector $\{\lambda\}$ must be solved simultaneously. For simplicity the aforementioned equations can be expressed as

$$[Mc]\begin{Bmatrix} \ddot{q} \\ \lambda \end{Bmatrix} = \{Q\} \tag{5.1}$$

where $[Mc]$ is mixed mass matrix of the system

$$[Mc] = \begin{bmatrix} M & -J_i^T \\ J_i & 0 \end{bmatrix} \qquad (i = 1, 2, 3) \tag{5.2}$$

and $\{Q\}$ is the mixed generalized forces

$$\{Q\} = \begin{Bmatrix} -[K]\{q\} - [\dot{M}]\{\dot{q}\} + \left\langle \dfrac{\partial T}{\partial \{q\}} \right\rangle^T + \{Q^{appl.nc}\} \\ -[\dot{J}_i]\{\dot{q}\} \end{Bmatrix} \tag{5.3}$$

Recalling the process of derivation of $[Mc]$ and $\{Q\}$ we find $[Mc]$ is not a constant matrix but a function of generalized coordinates $\{q\}$ and time t, while the mixed generalized force varies with the generalized coordinates $\{q\}$, the generalized velocity $\{\dot{q}\}$ and time t, all of which contribute to the nonlinearity of equations of motion for the system. Equation 5.1 can be solved by numerical integration algorithms with associated initial position and velocity vectors.

For a meaningful physical system where constraints are independently configured, the mixed mass matrix $[Mc]$ possesses full rank so that it is not singular and therefore invertible.

Multiplying both sides of equation 5.1 by $[Mc]^{-1}$ we have the solution

$$\begin{Bmatrix} \ddot{q} \\ \lambda \end{Bmatrix} = [Mc]^{-1}\{Q\} \tag{5.4}$$

further we can obtain $\{\lambda\}$

$$\{\ddot{q}\} = [B_q]\,[Mc]^{-1}\{Q\} \tag{5.5}$$

$$\{\lambda\} = [B_\lambda]\,[Mc]^{-1}\{Q\} \tag{5.6}$$

where $[B_q]$ and $[B_\lambda]$ are transformation matrices.

Once the generalized acceleration vector $\{\ddot{q}\}$ is computed, the position and velocity vectors at the next time step can be found by direct numerical integration. Here we resort to the Runge-Kutta algorithm, which demonstrates higher numerical stability in dealing with numerical integration.

Assuming

$$\{\ddot{q}\} = f(t, \{q\}, \{\dot{q}\}) \tag{5.7}$$

where $f(t,\{q\},\{\dot{q}\}) = [B_q]\,[Mc]^{-1}\{Q\}$, then the recursive formula for $\{q\}$ and $\{\dot{q}\}$ can be expressed as

$$\{q\}_{i+1} = \{q\}_i + h\left[\{\dot{q}\}_i + \frac{h}{6}(a_{1i} + a_{2i} + a_{3i} + a_{4i})\right] \tag{5.8}$$

$$\{\dot{q}\}_{i+1} = \{\dot{q}\}_i + \frac{h}{6}(a_{1i} + 2a_{2i} + 2a_{3i} + a_{4i}) \tag{5.9}$$

where h is the time step and

$$a_{1i} = f(t_i,\ \{q\}_i,\ \{\dot{q}\}_i)$$

$$a_{2i} = f\left(t_i + \frac{h}{2},\ \{q\}_i + \frac{h}{2}\{\dot{q}\}_i,\ \{\dot{q}\}_i + \frac{h}{2}a_{1i}\right)$$

$$a_{3i} = f\left(t_i + \frac{h}{2},\ \{q\}_i + \frac{h}{2}\{\dot{q}\}_i + \frac{h^2}{4}a_{1i},\ \{\dot{q}\}_i + \frac{h}{2}a_{2i}\right)$$

$$a_{4i} = f\left(t_i + h,\ \{q\}_i + h\{\dot{q}\}_i + \frac{h^2}{2}a_{2i},\ \{\dot{q}\}_i + ha_{3i}\right)$$

The initial conditions necessary for the solution are

$$\{q\} = \{q\}\Big|_{t=0} \quad \text{and} \quad \{\dot{q}\} = \{\dot{q}\}\Big|_{t=0} \tag{5.10}$$

From the Lagrangian multipliers calculated in equation 5.6, the generalized constraint forces can be computed as

$$\{Q^{cons}\} = [J_i]^T \{\lambda\} \tag{5.11}$$

As mentioned previously, the constraint conditions described by equation 4.60 and equation 4.64 have to be satisfied all the time. However, the method of direct numerical integration will inevitably cause accumulation of errors because the parameters of motion are updated recursively, during which the data at the current time step are based on those of last one. Sometimes the error may become so big that the constraint conditions will not hold. So at every time step we have to check if the following condition is met:

$$\|C_i(\{q\})\| \leq \epsilon_c \qquad (i = 1, 2, 3) \tag{5.12}$$

where $\|C_i(\{q\})\|$ is the norm of constraint vector $C_i(\{q\})$ and ϵ_c is the constraint error tolerance.

In case of violation we have to adjust the time step h until the inequality in 5.12 holds.

5. 2 Determination of initial conditions

As we discussed in the previous section, the deployment of the system is divided into two stages with different governing equations of motion and constraint conditions. Now we shall figure out the initial conditions for each stage.

5. 2. 1 Initial conditions for the first stage

5. 2. 1. 1 Initial position vector

The first step to solve the equations of motion is to find the initial position $\{q\}\Big|_{t=0}$ and velocity $\{\dot{q}\}\Big|_{t=0}$ of the system. Assuming α_1 is known as α_0 and there is no deformation for both the leaf and the link at the start of deployment.

Then

$$\{e_1\}\Big|_{t=0} = \{0\} \tag{5.13}$$

with a size of 6 by 1.

$$\{e_2\}\Big|_{t=0} = \{0\} \tag{5.14}$$

with a size of 3 by 1.

From equations 4.53, 4.54 and 4.57 we can obtain

$$l_1\cos\alpha_0 - R_2^x\Big|_{t=0} = 0 \tag{5.15}$$

$$l_1\sin\alpha_0 - R_2^y\Big|_{t=0} = 0 \tag{5.16}$$

and

$$l_3\cos\alpha_2\Big|_{t=0} + R_2^x\Big|_{t=0} = 0 \tag{5.17}$$

Solving these three equations leads to the following initial positions of point O'' and angle α_2,

$$R_2^x\Big|_{t=0} = l_1\cos\alpha \tag{5.18}$$

$$R_2^y\Big|_{t=0} = l_1\sin\alpha_0 \tag{5.19}$$

and

$$\alpha_2\Big|_{t=0} = \text{acos}\Big(-\frac{l_1}{l_3}\cos\alpha_0\Big) \tag{5.20}$$

So the initial position vector is

$$\{q\}\Big|_{t=0} = \begin{pmatrix} 0 \\ 0 \\ \alpha_0 \\ \{0\} \\ l_1\cos\alpha \\ l_1\sin\alpha_0 \\ \text{acos}\Big(-\frac{l_1}{l_3}\cos\alpha_0\Big) \\ \{0\} \end{pmatrix} \tag{5.21}$$

5. 2. 1. 2 Initial velocities

In the same way as the initial position, the initial velocities $\{\dot{q}\}\big|_{t=0}$ must also meet the constraint conditions at velocity level described by equation 4.61

$$[J_1]\{\dot{q}\}\big|_{t=0} = \{0\} \tag{5.22}$$

If the system is stationary at the beginning of deployment, which means there exist no initial velocity input for both rigid motion and deformation, then

$$\{\dot{q}\}\big|_{t=0} = \{0\} \tag{5.23}$$

If there exists an input velocity V_0 in the negative Y direction at joint H, the generalized initial velocities can be decided as follows:

First, at the initial moment no deformation and hence no velocities of deformation are induced. So for the leaf

$$\{\dot{e}_1\}\big|_{t=0} = \{0\} \tag{5.24}$$

with a size of 6 by 1, and for the link

$$\{\dot{e}_2\}\big|_{t=0} = \{0\} \tag{5.25}$$

with a size of 3 by 1 .

From equations 5.15 to 5.17 we can arrive at

$$-l_1\dot{\alpha}_0\sin\alpha_0 - \dot{R}_2^x\big|_{t=0} = 0 \tag{5.26}$$

$$l_1\dot{\alpha}_0\cos\alpha_0 - \dot{R}_2^y\big|_{t=0} = 0 \tag{5.27}$$

and

$$-l_3\dot{\alpha}_2\big|_{t=0}\sin\alpha_2\big|_{t=0} + \dot{R}_2^x\big|_{t=0} = 0 \tag{5.28}$$

Differentiation of both sides of equation 4.58 with respect to time t while considering u_{22} and $\dot{u}_{22}$ as vanishing leads to

$$\dot{r}_H^y\big|_{t=0} = \dot{R}_2^y\big|_{t=0} + l_3\dot{\alpha}_2\big|_{t=0}\cos\alpha_2\big|_{t=0} = V_0 \tag{5.29}$$

Combining equation 5.26 with equation 5.29, we get the following initial velocities:

$$\dot{\alpha}_0 = \frac{\sin\alpha_2\big|_{t=0}}{\sin\alpha_2\big|_{t=0}\cos\alpha_0 - \cos\alpha_2\big|_{t=0}\sin\alpha_0}\frac{V_0}{l_1}$$
$$= \frac{\sin\alpha_2\big|_{t=0}}{\sin(\alpha_2\big|_{t=0} - \alpha_0)}\frac{V_0}{l_1} \tag{5.30}$$

$$\dot{R}_2^x\big|_{t=0} = \frac{-\sin\alpha_0\sin\alpha_2\big|_{t=0}}{\sin(\alpha_2\big|_{t=0} - \alpha_0)}V_0 \tag{5.31}$$

$$\dot{R}_2^y\big|_{t=0} = \frac{\cos\alpha_0\sin\alpha_2\big|_{t=0}}{\sin(\alpha_2\big|_{t=0} - \alpha_0)}V_0 \tag{5.32}$$

and

$$\dot{\alpha}_2\big|_{t=0} = \frac{-\sin\alpha_0}{\sin(\alpha_2\big|_{t=0} - \alpha_0)}\frac{V_0}{l_3} \tag{5.33}$$

5. 2. 2 Initial conditions for the second stage

At the end of the first stage, the system reaches position $\{q_F\}$ with velocity $\{\dot{q}_F\}$, which can not be used as initial conditions directly for the second stage because there exists a violation of constraint conditions at the velocity level. As we assumed from Figure 4.1, joint H moves to point S and stops there.

Then we make the following assumptions:

(a) There is no loss of energy during the impact. So the totality of the kinetic and potential energy of the system remains constant.

(b) The velocities change instantaneously to fit the constraint conditions at velocity level.

(c) The system is still positioned at $\{q_F\}$ after the impact. So the potential energy is unchanged.

Based on these assumptions we obtain the initial position for the second stage

$$\{q_H\} = \{q_F\} \tag{5.34}$$

The kinetic energy is

$$\begin{aligned} T &= \frac{1}{2}\{\dot{q}_H\}^T[M]\{\dot{q}_H\} \\ &= \frac{1}{2}\{\dot{q}_F\}^T[M]\{\dot{q}_F\} \end{aligned} \tag{5.35}$$

Similarly, the constraint conditions at velocity level can be derived as

$$\dot{u}_2\Big|_H \cos\alpha_1\Big|_H - (l_1 + u_2\Big|_H)\dot{\alpha}_1\Big|_H \sin\alpha_1\Big|_H - \dot{R}_2^x\Big|_H = 0 \tag{5.36}$$

$$\dot{u}_2\Big|_H \sin\alpha_1\Big|_H + (l_1 + u_2\Big|_H)\dot{\alpha}_1\Big|_H \cos\alpha_1\Big|_H - \dot{R}_2^y\Big|_H = 0 \tag{5.37}$$

$$\dot{u}_5\Big|_H \cos\alpha_2\Big|_H - (l_3 + u_5\Big|_H)\dot{\alpha}_2\Big|_H \sin\alpha_2\Big|_H + \dot{R}_2^x\Big|_H = 0 \tag{5.38}$$

and

$$\dot{u}_5\Big|_H \sin\alpha_2\Big|_H + (l_3 + u_5\Big|_H)\dot{\alpha}_2\Big|_H \cos\alpha_2\Big|_H + \dot{R}_2^y\Big|_H = 0 \tag{5.39}$$

Then we assume only the rigid velocities $\dot{R}_2^x\Big|_H$, $\dot{R}_2^y\Big|_H$, $\dot{\alpha}_1\Big|_H$ and $\dot{\alpha}_2\Big|_H$ and elastic velocity $\dot{u}_5\Big|_H$ are variable. So the redistribution of velocities can be calculated by solving equations 5.36 to 5.39 numerically.

5. 3 Stress analysis

By solving the differential-algebraic equations of motion of the system we can obtain the generalized coordinates $\{q\}$ and therefore the elastic coordinates $\{e_1\}$ for the leaf and $\{e_2\}$ for the link. Then the displacement field and distribution of stress of an arbitrary element on either body of the system can be obtained. Taking into account the assumptions of basic beam theory, we neglect the shear stress here.

As already indicated, the moment at an arbitrary point on element j of body i can be expressed as

$$M_i = E_i I_i v''$$

Substituting equation 4.41 into it leads to

$$M_i = E_i I_i \langle 0 \quad 1 \rangle [N''] \{d_j\} \tag{5.40}$$

in which

$$[N''] = \frac{1}{l^2} \begin{bmatrix} 0 & 0 & 0 & 0 & 0 & 0 \\ 0 & 6+12\eta & l(-4+6\eta) & 0 & 6-12\eta & l(6\eta-2) \end{bmatrix}$$

where $\eta = \dfrac{x}{l}$.

The axial force at an arbitrary point on element j of body i is

$$N_i = E_i A_i u'$$

Substituting equation 4.40 into it leads to

$$N_i = E_i A_i \langle 1 \quad 0 \rangle [N'] \{d_j\} \tag{5.41}$$

in which

$$[N'] = \frac{1}{l} \begin{bmatrix} -1 & 0 & 0 & 1 & 0 & 0 \\ 0 & -6\eta+6\eta^2 & l(1-4\eta+3\eta^2) & 0 & 6\eta-6\eta^2 & l(3\eta^2-2\eta) \end{bmatrix}$$

The strain of a material point with a distance of y from the neutral axis of beam element j on body i can be derived as

$$\varepsilon = u' - yv''$$

Considering the expressions of u' and v'', the strain becomes

$$\varepsilon = \Big(\langle 1 \quad 0 \rangle [N'] - y \langle 0 \quad 1 \rangle [N''] \Big) \{d_j\} \tag{5.42}$$

The stress at the same point is

$$\sigma = E_i \varepsilon$$

$$= E_i \Big(\langle 1 \quad 0 \rangle [N'] - y \langle 0 \quad 1 \rangle [N''] \Big) \{d_j\} \tag{5.43}$$

The maximum stress on the cross-section passing through the point is

$$\sigma_{max} = E_i \Big(\langle 1 \quad 0 \rangle [N'] - \frac{b}{2} \langle 0 \quad 1 \rangle [N''] \Big) \{d_j\}$$

or

$$\sigma_{max} = E_i\left(\langle 1 \quad 0 \quad \rangle[N'] + \frac{b}{2}\langle 0 \quad 1 \quad \rangle[N'']\right)\{d_j\} \tag{5.44}$$

where b is the height of the cross-section.

5. 4 Numerical process and programming

5. 4. 1 Simulation of the opening of a deformable system

As already mentioned, the deployment of an umbrella can be divided into two stages governed by different dynamic equations because of the different constraint conditions attached. The first stage characterized by equation 4.87 describes the opening under given initial force or velocity conditions up to the moment of full deployment. Equation 4.118 deals with the vibration induced at the second stage when the umbrella is fully opened.

The flow chart of programming for the first stage is presented in Figure 5.1. The procedure is detailed as follows:

(a) Input of the necessary data and definition of initial conditions

The data include those of geometry, material properties, initial configuration of the system and force or initial velocity at joint H. In this FE model, each component is treated as a uniform beam so that the lengths, cross-sectional information and the position of joints of each body are necessary. The modulus of elasticity and the mass density of the material are required for each component of the system. The force or initial velocity at joint H is the source of power for the opening of the umbrella.

Considering the initial configuration and initial velocity at joint H, we can then figure out the initial position $q|_{t=0}$ and initial velocities $\dot{q}|_{t=0}$ by resorting to equation 5.21 to equation 5.33.

(b) Constituting the governing equations of motion

At this step we have to compute the mass and stiffness matrices at element level and assemble them into a system mass matrix $[M]$ and a stiffness matrix $[K]$, respectively. At the same time we need to calculate the time and spatial derivatives of the system mass matrix $[M]$. In order to form the governing equations of motion the constraint Jacobian matrix is also evaluated according to the corresponding constraint conditions. From the formulation of the equations of motion we know that the system mass matrix varies with the generalized coordinates $\{q\}$ and the generalized forces are a function of both $\{q\}$ and the generalized velocities $\{\dot{q}\}$, so that they have to be updated at every time step. The system stiffness matrix is constant and can be saved for recall whenever necessary. Once the mixed mass matrix $[Mc]$ and the mixed generalized forces $\{Q\}$ are computed, we can then assemble the nonlinear differential-algebraic equation 4.87.

(c) Solving the differential-algebraic equations

By utilizing equation 5.4 we can solve equation 4.87 for the generalized accelerations $\{\ddot{q}\}$ and the vector of Lagrangian multipliers $\{\lambda\}$. Further, the Runge-Kutta algorithm of direct numerical integration is adopted to find the new $\{q\}$ and $\{\dot{q}\}$, which will be updated for next time increment if the constraint conditions hold. Otherwise, the time step h_1 has to be diminished to obtain a smaller error of accumulation until the requirements are met. The next step is to carry out stress analysis with the updated elastic coordinates. At every time step we can work out the generalized constraint forces by the product of the transposed Jacobian and the vector of Lagrangian multipliers $\{\lambda\}$.

Steps (b) and (c) continue iteratively until the moment of full deployment, which means the end of the first stage and the beginning of the second one. Then we output the values of $\{q\}$ and $\{\dot{q}\}$ and go on to the second stage.

(d) Analysis of vibration induced at full deployment

From the flow chart for the second stage shown in Figure 5.2 we can see the numerical procedure is fundamentally similar to that of the first stage except that we have to call up the output data $\{q\}$ and $\{\dot{q}\}$ of the first stage to calculate the initial conditions for solving equation 4.118 with a different constraint Jacobian. The second stage finishes when the simulation time T is due.

5. 4. 2 Simulation of the opening of a rigid-body system

If the deformation of the components is neglected, the FE model turns into a rigid-body model with all elastic coordinates constrained. The flow chart and solving strategy for this case are basically the same as the first stage outlined in Section 5. 4. 1. Therefore we do not need to detail them here.

Following the aforementioned procedure we can evaluate the variation of kinetic and dynamic parameters with respect to time. These results will be validated by the formulation of rigid-body dynamics that can function as references for the FE model of the deformable system.

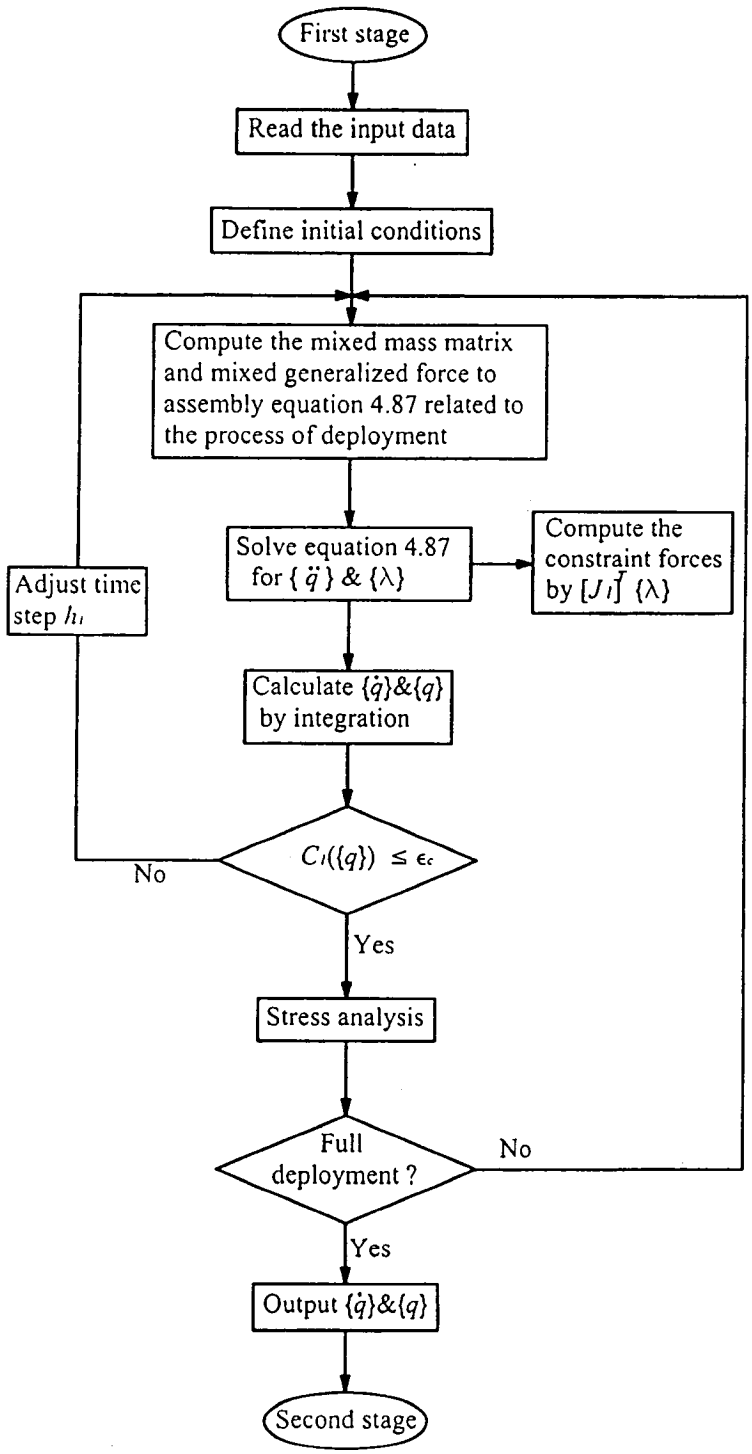

Figure 5.1 Flow chart for the first stage

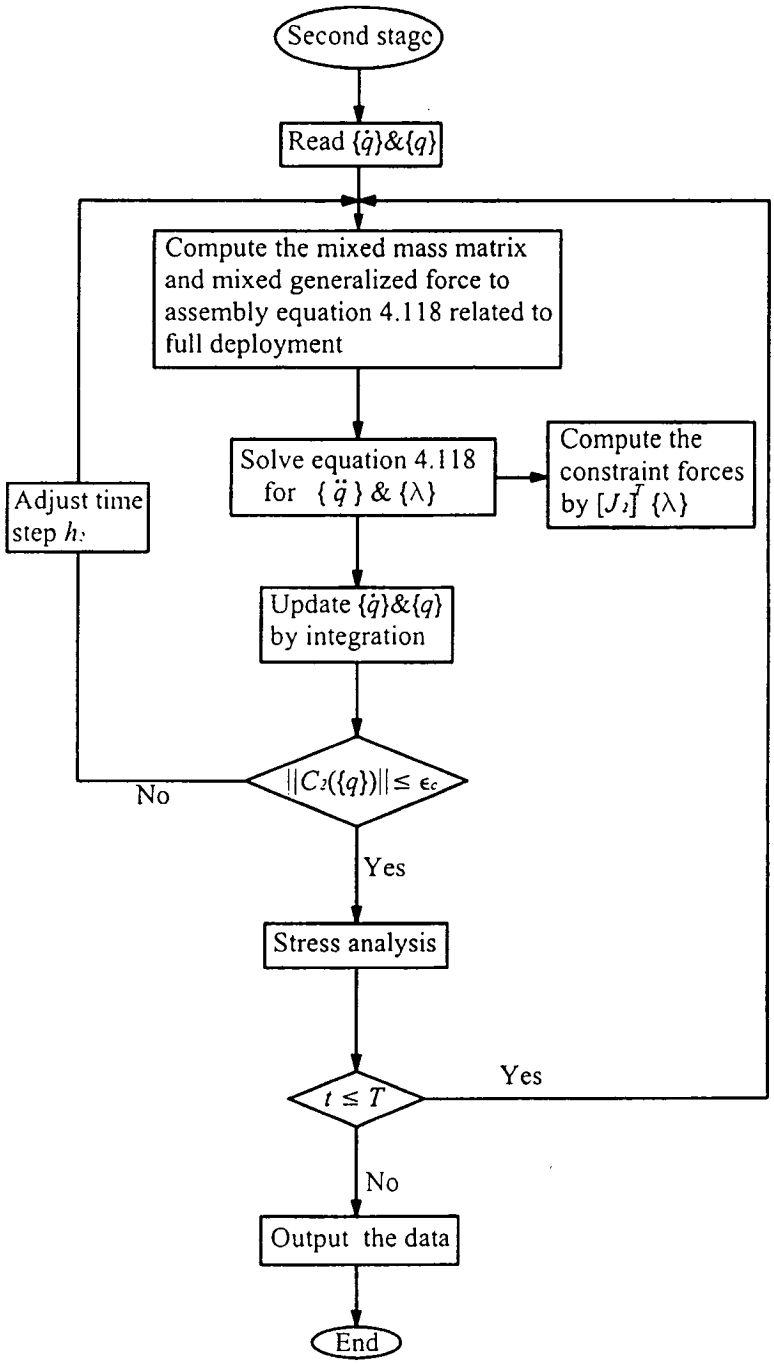

Figure 5.2 Flow chart for the second stage

Chapter 6

Results and Discussions

In this chapter we first solve the derived governing equations of motion for the 3-element FE deformable model to simulate the whole opening process of an umbrella. Then we present some results of finely-meshed FE models and those of rigid-body models for the sake of comparison.

The shared data concerning material and its properties and the dimensions of the configuration of the system are given as follows:

Material:

Al 7075 T6

Properties:

$$\rho_1 = \rho_2 = 2.77 \times 10^3 \text{ kg/m}^3$$

$$\sigma_y = 500 \text{ MPa}$$

$$E_1 = E_2 = 72.0 \text{ GPa}$$

Dimensions:

$$l_1 = l_2 = l_3 = 0.5 \text{ m}$$

$$A_1 = A_2 = 0.01 \times 0.01 \text{ m}^2$$

Initial velocity at joint H :

$$V_0 = -0.2 \text{ m/s}; -0.5 \text{ m/s}; -1.0 \text{ m/s}; -2.0 \text{ m/s}.$$

Initial position:

$$\alpha_1 = \alpha_0 = \frac{49}{100}\pi$$

Angle at full deployment:

$$\alpha_1 = \frac{1}{12}\pi$$

6. 1 Simulation of the opening process with a 3-element FE model

As discussed before, the 3-element model is composed of two elements placed on the leaf and one element on the link. The simulation starts from the beginning with the initial position $\alpha_1 = \frac{49}{100}\pi$ and the initial velocity $V_0 = -0.2$ m/s applied at joint H to the full deployment.

Figure 6.1 shows the time history of angle α_1, the rotation of the leaf, from which we can find at time t=0.2259s that joint H moves to point S when the system reaches full deployment at $\alpha_1 = \frac{1}{12}\pi$.

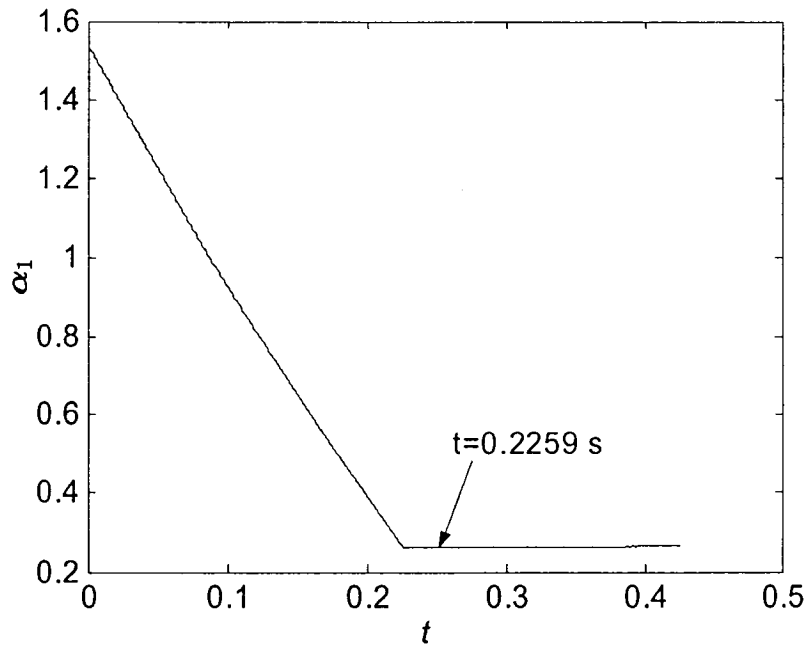

Figure 6.1 Variation of α_1 as a function of time

Figure 6.2 describes the variation of transverse displacement at the end point G on the leaf with respect to the moving frame $X'O'Y'$ up to the moment of full deployment, as is the first stage of opening. The deformation fluctuates with the time, and the maximum value is 0.665 mm occurring at 0.08s.

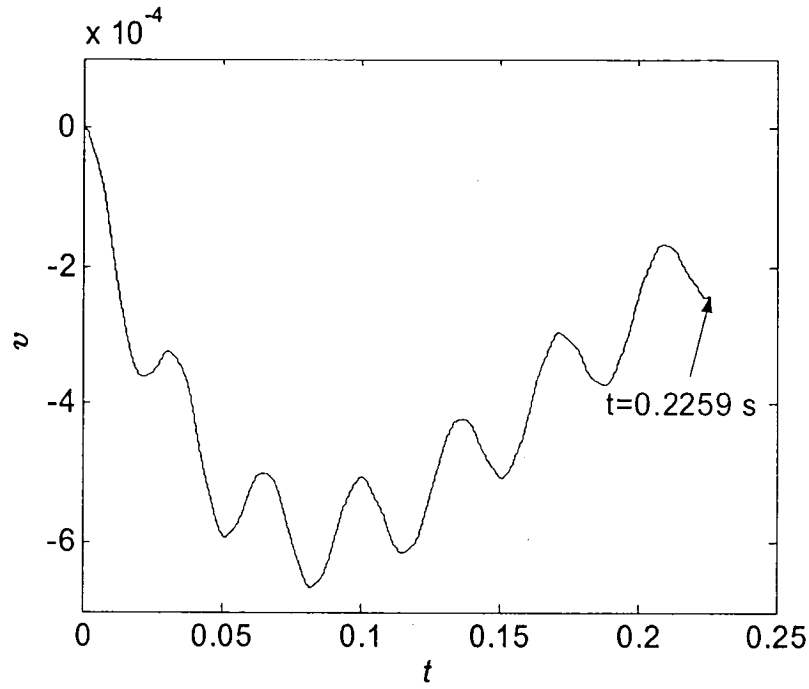

Figure 6.2 Transverse displacement at G in the first stage of opening

Figure 6.3 depicts the time history of maximum stresses on the leaf and link in the first stage. The maximum stresses occur at joint O'' on the leaf and at the center of the link. As can be seen, the stress on the link expressed by the solid line is smaller than that on the leaf.

As for the full process of opening, Figure 6.4 shows the significant vibration induced at full deployment in the second stage. The deformation changes periodically with an amplitude of as large as 60 mm and a cycle of about 0.05s. The system will vibrate perpetually with that constant amplitude because the external forces and damping effect are ignored.

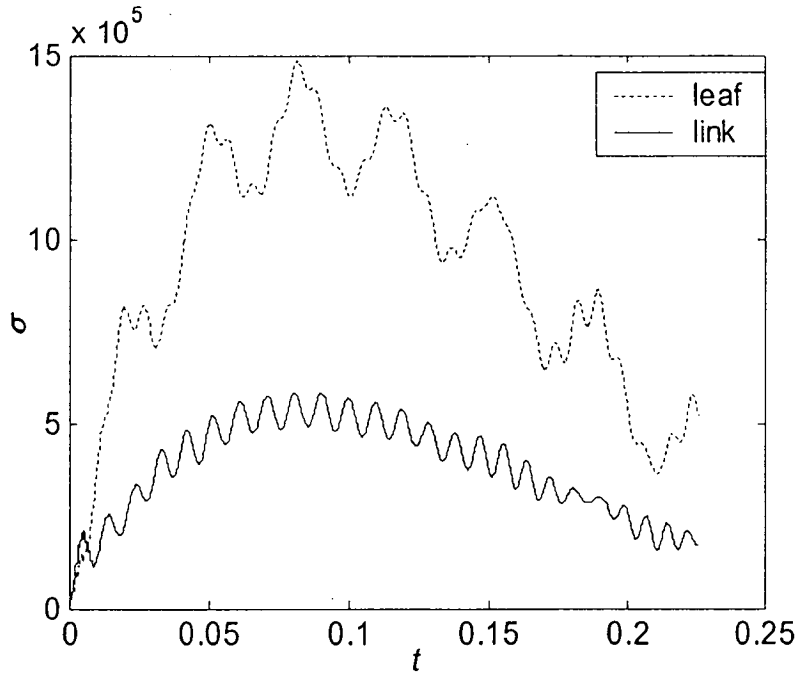

Figure 6.3 Variation of maximum stresses on the leaf and link

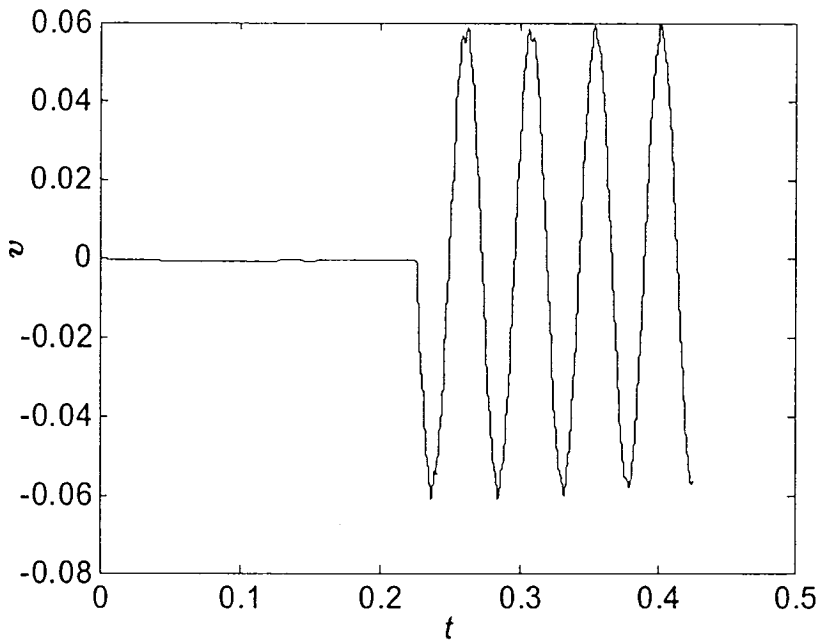

Figure 6.4 Transverse displacement at G including the second stage

The stresses initiated from the deformation at point O'' on the leaf and the center of the link are shown in Figure 6.5 and Figure 6.6, respectively. The variation of stress with time also displays characteristics of periodicity and the magnitude is comparably high due to the larger deformation in the second stage on each component. In the same way as in the first stage, a much higher stress level is produced on the leaf.

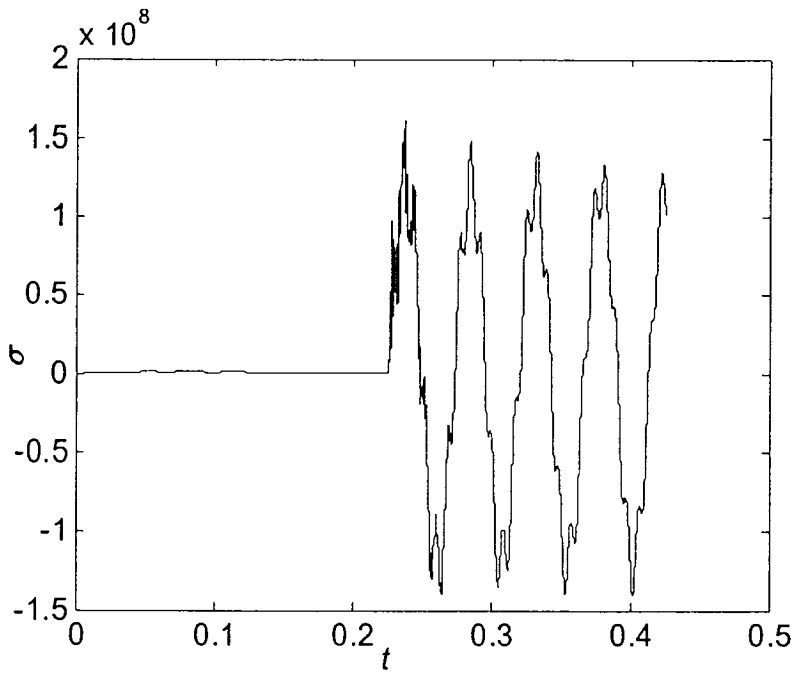

Figure 6.5 Stress variation as a function of time at point O'' on the leaf

Figure 6.7 and Figure 6.8 supply an insight into the dynamic response induced in the deployment of an umbrella by plotting the successive deformed shapes at several moments. In Figure 6.7 we can easily feel the deformation and vibration in the second stage after the time 0.2259s. However, little information about deformation is displayed before that time because it is comparatively small. In order to scrutinize the responses in the first stage, we simply magnify the transverse deformation of each body by two hundred times to form the deformed shapes in Figure 6.8, which show the deformation of the system clearly.

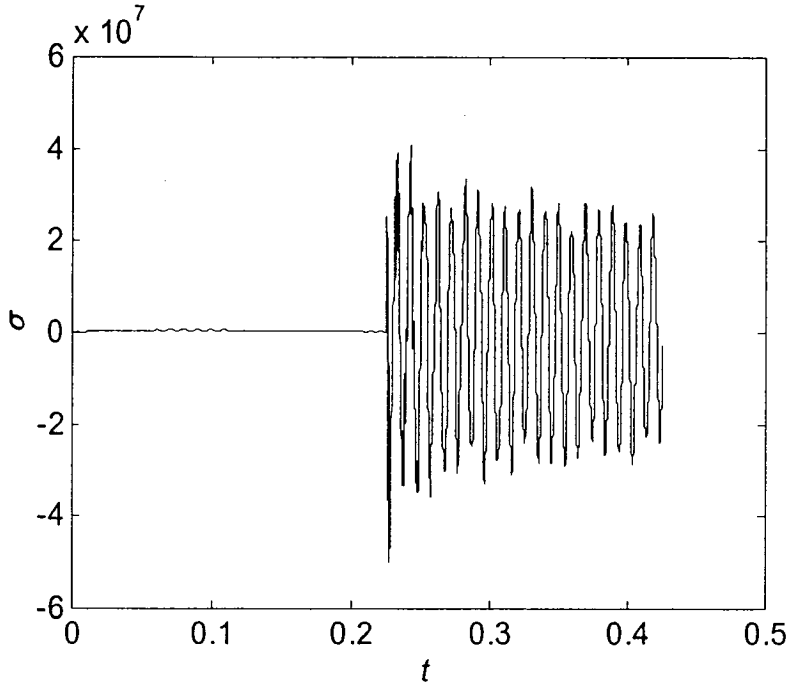

Figure 6.6 Stress variation as a function of time at the center of the link

At this point we can conclude that in the deployment of the system the leaf experiences larger deformation than the link, and that at full deployment the significant periodical oscillations are excited both on the leaf and the link, which produce relatively large deformation and stresses especially on the leaf. Then we can deduce that if the initial velocity V_0 or input energy is too high it will induce large deformation on the leaf at full deployment. In this case the governing equations of motion previously derived and based on the assumption of small deformation are no longer applicable and many other factors such as inertia of rotation and shortening effect of projection of the beams or effect of geometrical stiffening should be taken into account in the formulation in order to simulate the reality.

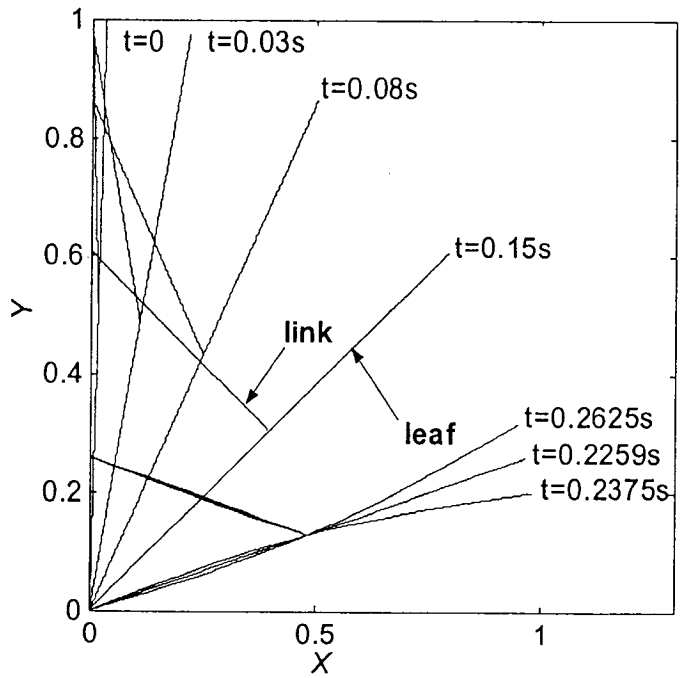

Figure 6.7 Deformed shapes in the deployment of the system

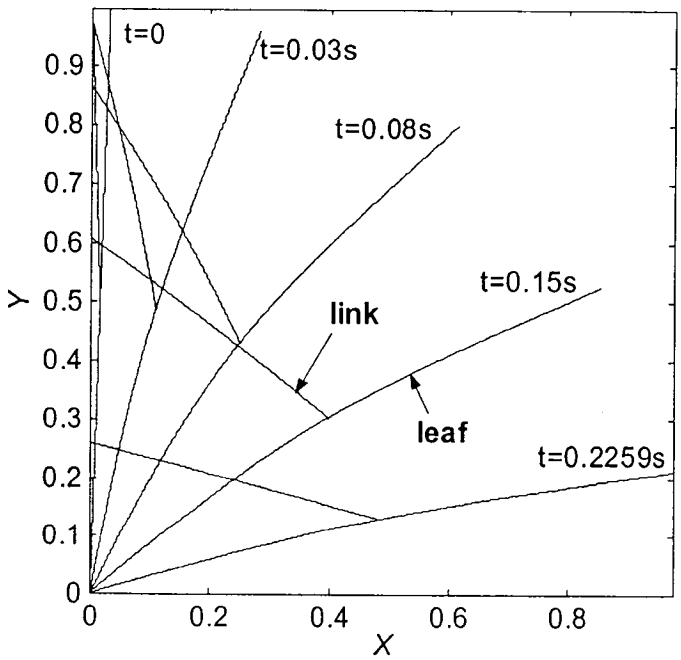

Figure 6.8 Magnified shapes of deformation in the first stage

6. 2 Comparison of results between 3-element and 6-element models

In order to present the figures clearly, we compare the results calculated in the first stage pertinent to 3-element and 6-element models. The 6-element FE model consists of four elements equally spaced on the leaf and two elements meshed in the same manner on the link. The system is excited for motion by applying initial velocity $V_0 = -1.0\ \mathrm{m/s}$.

From Figure 6.9 we can recognize that the relations of α_1 versus time coincide with each other and display characteristics of linearity. Both models take the same time (0.0452s) to reach full deployment.

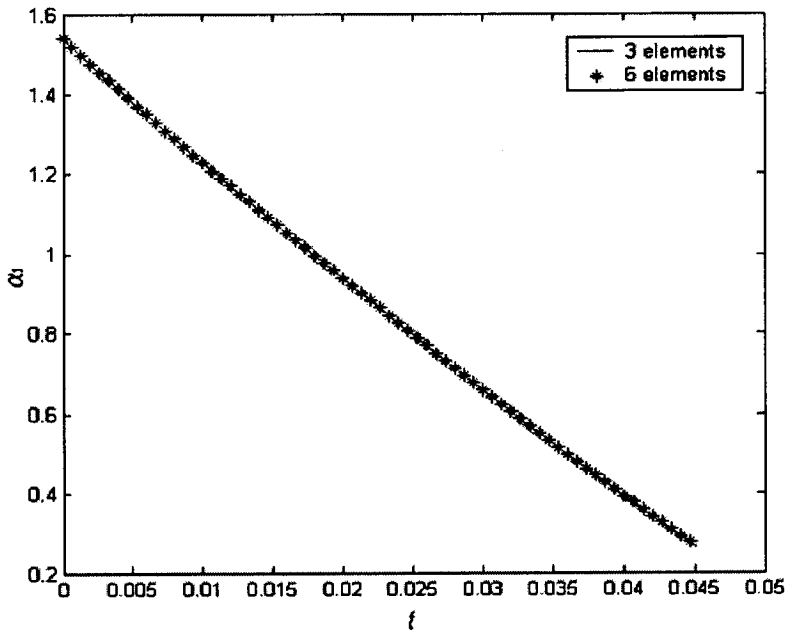

Figure 6.9 Time histories of α_1 for 3-element and 6-element models

In Figure 6.10 the two curves depict the transverse deformation at end point G concordantly, except that a small diversion exists at the end of the stage.

Figure 6.11 displays the stress variation at joint O'' on the leaf, in which the stress for the 6-element model is a little higher than that for the 3-element model as a whole.

However, the 3-element or 6-element model can sufficiently describe the dynamic behavior of the system with an acceptable burden of computation.

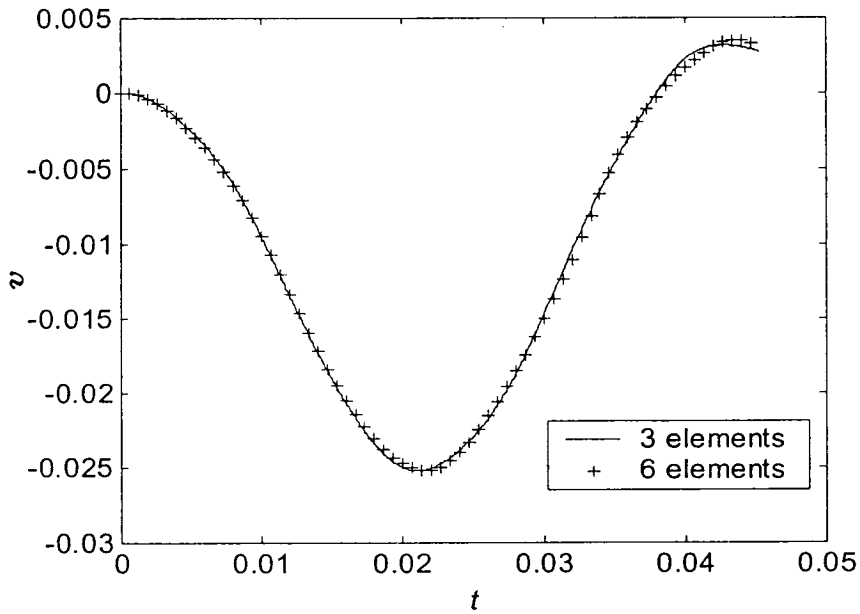

Figure 6.10 Transverse deformation at G for 3-element and 6-element models

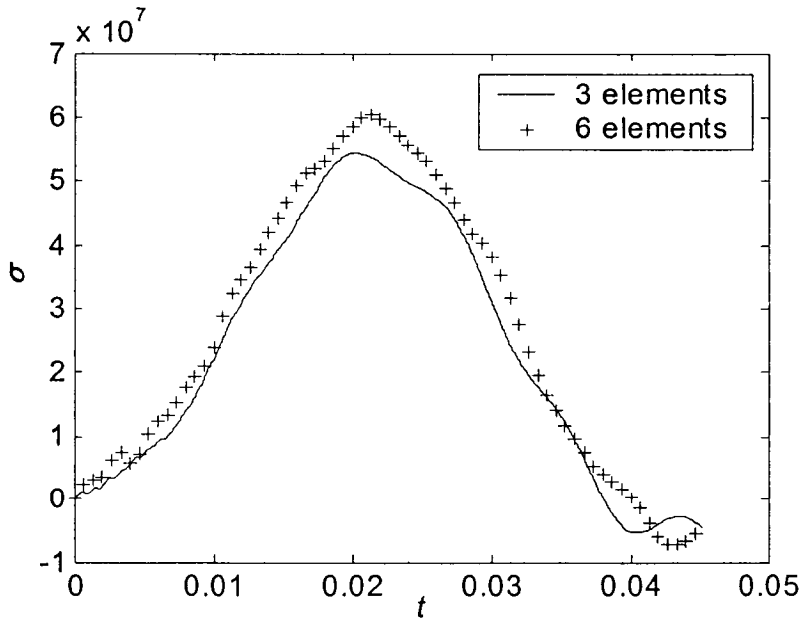

Figure 6.11 Stress variation at O'' on the leaf for 3-element and 6-element models

6. 3 Comparison of the results between deformable and rigid FE models

Comparison of the kinematic aspects between the deformable and rigid-body FE models relative to the constraint condition in Case 3 uncovers how the deformable FE model relates to the rigid FE model.

Figure 6.12 displays the relations of rotation α_1 versus time. From this we can see that the curve related to rigid FEA deviates a little downward from that of deformable FEA, which further reminds us of the probable shorter time taken to reach full deployment for the rigid FE model. This inference can be verified by calculating the time of deployment at the three different initial velocities as shown in Table 6.1. We can thus conclude that the deformation of the bodies will cause the delay of the deployment of the system, as becomes clearer at higher speeds at which more kinetic energy of the system is transformed to potential energy to support the larger deformation.

Figures 6.13 and 6.14 depict the time history of angular velocity and angular acceleration, respectively, of the leaf. Obvious deviation and fluctuation in the vicinity of the curves related to rigid FEA can be found for the deformable FE model at the velocity and acceleration levels. But they follow the same trend of variation with respect to time.

Therefore, the results calculated by the rigid-body FEA model with numerical stability can function as references for the deformable FEA models as a whole to verify its feasibility.

Table 6.1 Time of deployment for deformable and rigid model at different V_0

Initial velocity V_0 (m/s)	Time needed (s)		Time prolonged (s)
	Deformable FEA	Rigid FEA	
-0.5	0.09040	0.09033	0.00007
-1.0	0.04525	0.04517	0.00008
-2.0	0.02343	0.02259	0.00084

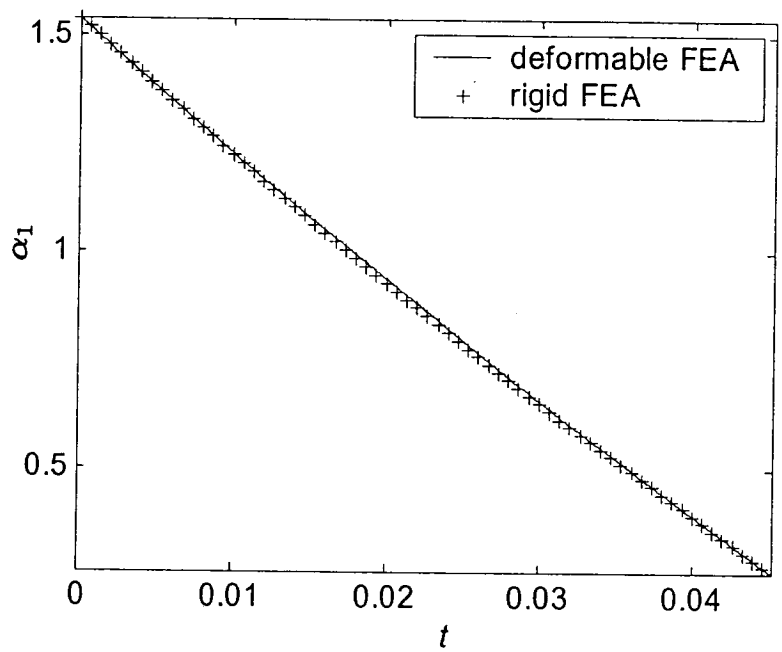

Figure 6.12 Relations of rotation α_1 versus time for deformable and rigid FEA

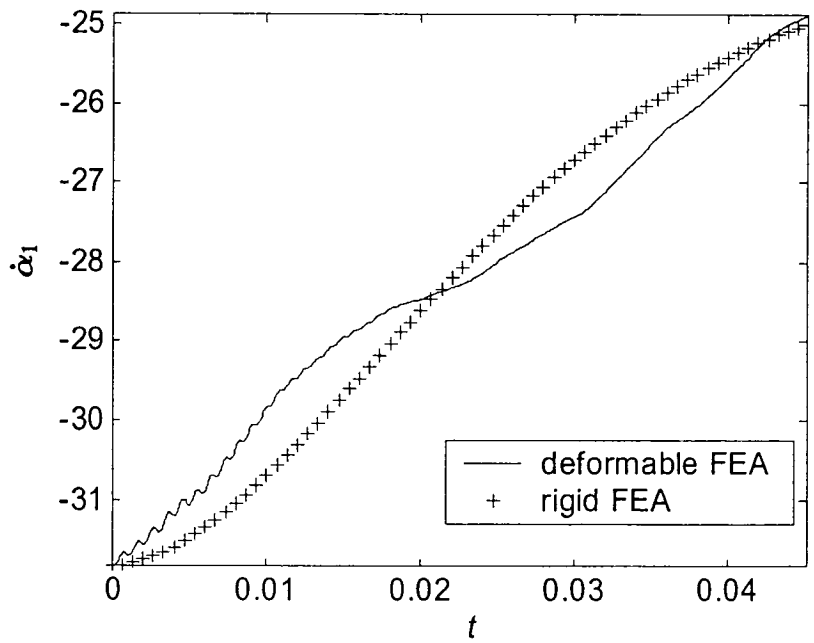

Figure 6.13 Relations of velocity $\dot{\alpha}_1$ versus time for deformable and rigid FEA

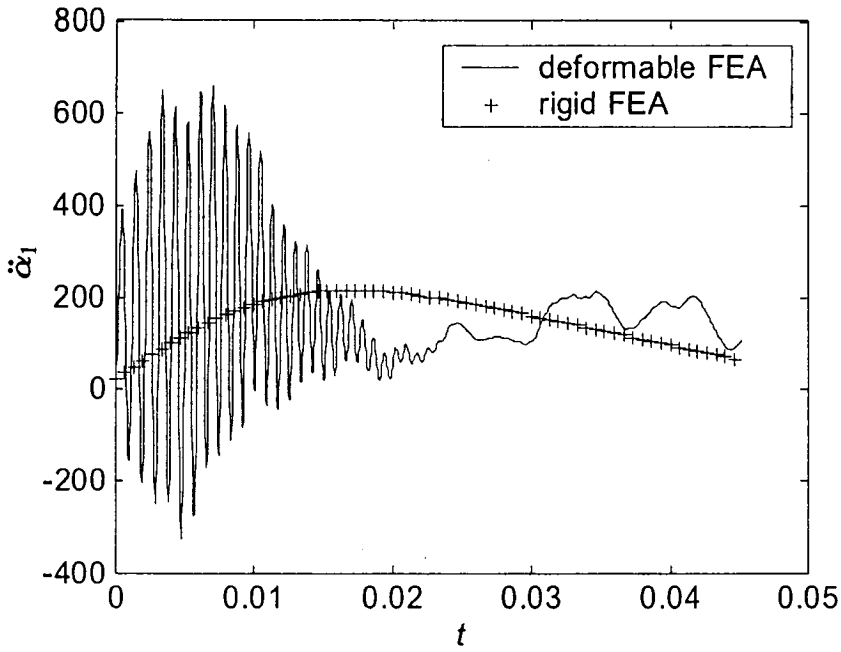

Figure 6.14 Relations of acceleration $\ddot{\alpha}_1$ versus time for deformable and rigid FEA

6. 4 Comparison of the results between rigid FEA and rigid dynamics

Figure 6.15 to Figure 6.17 show the time histories of position, velocity and acceleration respectively for the rigid FE model and the rigid dynamics model.

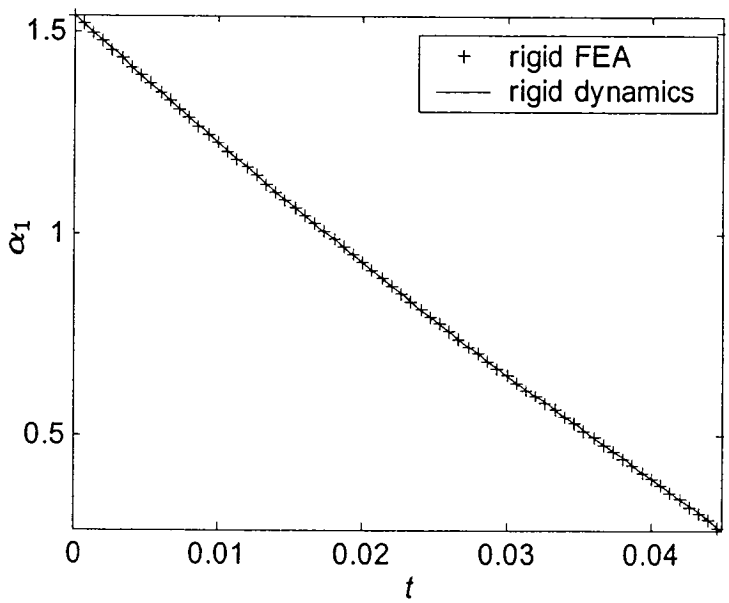

Figure 6.15 Time histories of α_1 for rigid FE model and rigid dynamics model

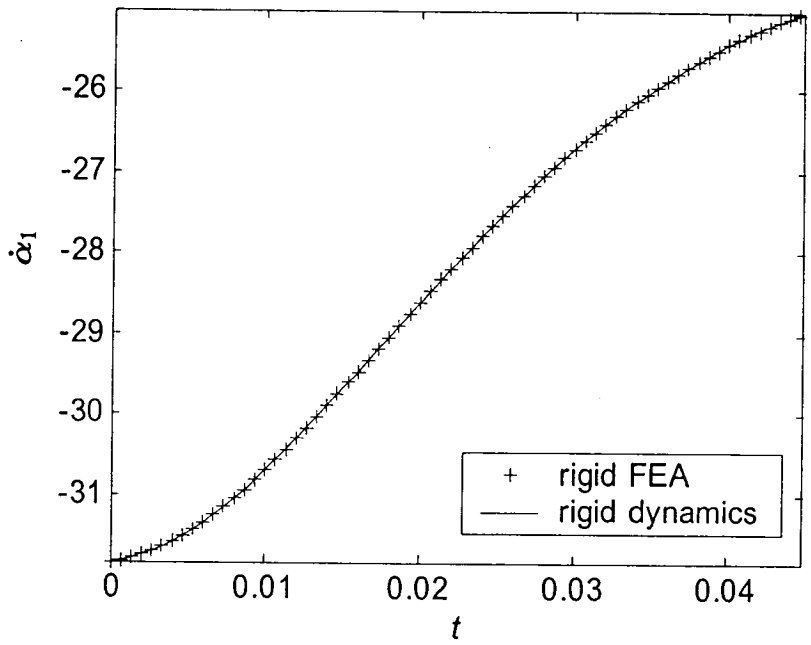

Figure 6.16 Time histories of $\dot{\alpha}_1$ for rigid FE model and rigid dynamics models.

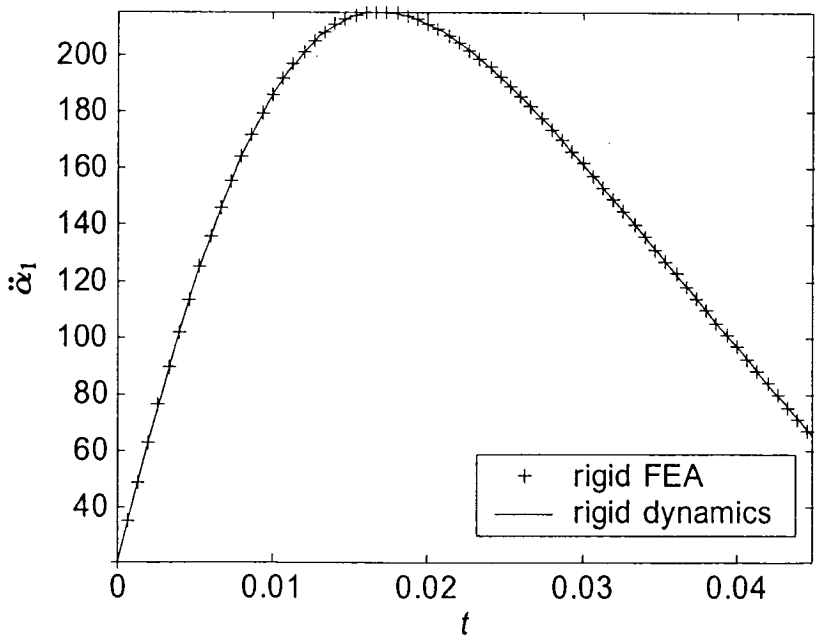

Figure 6.17 Time histories of $\ddot{\alpha}_1$ for rigid FE model and rigid dynamics model

From these figures we can see that the results computed by the rigid FE model coincide with those of rigid dynamics. So the rigid-body FE model with the constraint conditions of Case 3 is an exact, rigid model.

Chapter 7

Conclusions and Recommendations

7. 1 Conclusions

A deformable FE model has been developed to simulate the opening process of an umbrella, including the analysis of the vibration and stresses induced at full deployment without considering the gravity of the components of the system. Necessary assumptions such as small deformation, no damping and no friction were made to limit the scope of this work. The elastic deformation of each member was modeled by FEM, in which both longitudinal and transverse displacements were considered and the component along the axis was linear. Based on the Euler-Bernoulli beam theory, the governing equations of motion were derived using constrained Lagrangian generalized coordinates, which consist of rigid coordinates describing the rigid-body motions and elastic coordinates related to deformation of the members.

Recalling Chapter 3, we know that the body-fixed moving frames introduce additional constraints that delete the rigid-body mode of the assumed displacement field so that the position of an arbitrary point on a body can be located by the generalized coordinates of the system with respect to the inertial frame. Then in Chapter 4 the kinetic and potential energy of the elements, members and the system as a whole were formulated successively, and at the same time the variable mass matrices and constant stiffness at each level were derived. By virtue of the different constraint conditions, the process of deployment was divided into two stages representing motion before and after full opening. In order to validate the deformable FE model, a pure rigid-body mode was proposed with the deformation of all members ignored. Then by invoking Lagrange's equation with multipliers we arrived at the governing equations of motion in differential-algebraic form, each term of which was deduced and expressed in detail. We can find the

coupling effects of inertia in the mass matrix of the system, which is dependent on the generalized coordinates of the system, and recognize that the generalized forces vary with both the generalized coordinates and the generalized velocities. Therefore, the governing equations of motion display highly nonlinearity, which can only be solved by method of direct numerical integration. As for the validation of finite element models, the closed-form governing equations of motion for the rigid-body model with two constrained generalized coordinates were formulated by the way of rigid-body dynamics, the results of which will act as references for the finite element method.

Detailed strategies of solution and programming were presented in Chapter 5. The Runge-Kutta algorithm was used to perform the numerical integration while the corresponding constraint conditions were checked at every time step. The crucial step to simulate the dynamic behavior in the second stage is to figure out the related initial conditions. There we assumed that the occurrence of redistribution of velocities takes no time, so the initial position of the system is defined by the end of the first stage. The initial velocities were derived by a further assumption of energy conservation at full deployment. At each time step once the generalized coordinates are calculated we can implement the stress analysis with the elastic coordinates, a procedure similar to that of the structural FEA.

Numeric process and illustrative examples were presented in Chapter 6. A 3-element deformable model was utilized to simulate the whole process of the opening of an umbrella with specified material and geometrical properties. This umbrella was set in motion by applying an initial velocity at the sleeve or joint H. The solution revealed the shapes of deformation and hence variation of stresses for both the leaf and the link. In the process of opening, the leaf experienced larger deformation and stresses than the link, and at the full deployment, significant periodical vibration was induced on the leaf.

Comparison of the results for the 3-element model and the 6-element model showed that good agreement was achieved between them in kinematic and dynamic

aspects, and a more densely meshed model is not recommended because of the huge efforts of computation to be paid.

The coincidence of the results in kinematics at position, velocity and acceleration levels for the rigid FEA model and the rigid-body dynamics model demonstrated that the rigid FEA is an exact rigid-body model. Usually the results of a deformable FE model in kinematic aspects fluctuate about those of a rigid-body mode, which can therefore play as references to validate the deformable FE model.

From the elapsed time to reach full opening, it can be concluded that deformation of the components will delay the deployment, and that this becomes more significant at higher speeds. This phenomenon can be explained by the principle of energy conservation: less kinetic energy contributes to the motion as the deformation becomes larger.

As we can see from this research, the formulating process is based on the 2-body holonomic constraint model. However, this method can also be applicable to a more complicated nonholonomic system.

7. 2 Recommendations for further study

As mentioned before, this FE model was derived from the basic assumption of a small deformation in which the longitudinal deformation of the beams is linear and the rotation of inertia is negligible. However, if the initial input velocity V_o at the sleeve is too high the ensuing vibration and deformation on the leaf at full deployment will become very large, which obviously invalidates the base of the model. In this case, a nonlinear strain-displacement relation should be introduced to consider the effect of transverse deformation to the longitudinal displacement of beams, which is also called geometric stiffening or the shortening effect of projection. The centrifugal force at high speed will have a significant effect on the flexural stiffness of the beams, hence the stiffness matrix is no longer constant. In the meantime, the effect of inertial rotation of the beams has to

be taken into account because of the high speed of deformation that is induced at the instant of full deployment.

Further studies are also recommended to concentrate on the experiment to validate the developed FE model, the measures to weaken the ensuing vibration and deformation at full deployment of the umbrella antenna, failure analysis, and a simulation in three-dimensional configuration.

References

[1] Robert D. Cook, Concepts and Applications of Finite Element Analysis, John Wiley & Sons. Inc, 2001.

[2] H. Baruh, Analytical Dynamics, McGraw-Hill, 1999.

[3] Ray W. Clough and Joseph Penzien, Dynamics of Structures, McGraw-Hill, 1993.

[4] Edward J. Haug, Computer-Aided Kinematics and Dynamics of Mechanical Systems, Allyn and Bacon, 1989.

[5] Farid. M. L. Amirouche, Computational Methods in Multibody Dynamics, Prentice-Hall, Inc. 1992.

[6] Ahmed A. Shabana, Computational Dynamics, John Wiley & Sons. Inc, 1994.

[7] Ahmed A. Shabana, Dynamics of Multibody Systems, John Wiley & Sons. Inc, 1998.

[8] Rex J. Theodore and Ashitava Ghosal, Comparison of the Assumed Modes and Finite Element Models for Flexible Multilink Manipulators, The International Journal of Robotics Reseach, Vol. 14, No. 2, April 1995, pp. 91-111.

[9] K. H. Low and M. Vidyasagar, A Lagrangian Formulation of the Dynamic Model for Flexible Manipulator Systems, The Journal of Dynamic Systems, Measurement, and Control, Vol. 110/181, June 1988.

[10] Alessandro De Luca, Closed-Form Dynamic Model of Planar Multilink Lightweight Robots, IEEE Transactions on System, Man and Cybernetics, Vol. 21, No. 4, July/August 1991, pp.826-839.

[11] Jorge Martins and Miguel Ayala Botto, Modeling of Flexible Beams For Robotic Manipulators, Multibody System Dynamics, Vol. 7, 2002, pp.79-100.

[12] B. V. Viscomi and R. S. Ayre, Nonlinear Dynamic Response of Elastic Slider-Crank Mechanism, Journal of Engineering for Industry, February 1971, pp. 251-262.

[13] R. A. Laskin etc., Dynamical Equations of a Free-Free Beam Subject to Large Overall Motions, Journal of the Astronautical Sciences, Vol.31/Issue 4, 1983, pp.507-528.

[14] M. Geradin and D. Rixen, Mechanical Vibrations: Theory and Application to Structural Dynamics, 1997.

[15] Ji Oh Song and Edward J. Haug, Dynamic Analysis of Planar Flexible Mechanisms, Computer Methods in Applied Mechanics and Engineering, Vol. 24,1980, pp. 359-381.

[16] J. C. Simo and L. Vu-Quoc, On the Dynamics of Flexible Beams Under Large Overall Motion — The Plane Case: Part 1 & Part 2, Journal of Applied Mechanics, Vol. 53, 1986, pp. 849-863.

[17] I. Sharf, Nonlinear Strain Measures, Shape Functions and Beam Elements for Dynamics of Flexible Beams, Multibody System Dynamics, Vol. 3, 1999, pp. 189-205.

[18] Madeleine Pascal, Some Open Problems in Dynamic Analysis of Flexible Multibody Systems, Multibody System Dynamics, Vol. 5, 2001, pp. 315-334.

[19] R. G. Langlois and R. J. Anderson, Multibody Dynamics of Very Flexible Damped Systems, Multibody System Dynamics, Vol. 3, 1999, pp. 109-136.

[20] Ahmed A. Shabana, Flexible Multibody Dynamics: Review of Past and Recent Developments, Multibody System Dynamic, Vol. 1, 1997, pp. 189-222.

[21] Biggs, John M. , Introduction to Structural Dynamics, McGraw-Hill, 1964.

[22] M. Benati and A.Morro, Dynamics of Chain of Flexible Links, The Journal of Dynamic Systems, Measurement, and Control, Vol.110, December 1988, pp. 410-415.

[23] J. Kövecses, A Distributed Parameter Model for the Dynamics of Flexible-Link Robots, Journal of Robotic Systems, Vol. 15(5), 1998, pp. 281-298.

[24] P. B. Usoro etc. , A Finite Element/Lagrange Approach to Modeling Lightweight Flexible Manipulators, The Journal of Dynamic Systems, Measurement, and Control, Vol. 108, September 1986, pp. 198-205.

Appendix A

Mass Matrices and Jacobian Matrices

A.1 Mass matrix for each element

$$[M_1] = \rho_1 l_1 \begin{bmatrix} \frac{1}{3}l_1^2 + \frac{2}{3}l_1u_2 + \frac{1}{105}l_1^2\theta_1^2 & \frac{1}{30}l_1(l_1+u_2) & (-\frac{1}{30}\theta_1 + \frac{1}{20}\theta_2)l_1 & -\frac{1}{20}(l_1+u_2)l_1 & 0 & 0 & 0 \\ -\frac{1}{70}l_1^2\theta_1\theta_2 + \frac{1}{3}u_2^2 + \frac{1}{105}l_1^2\theta_2^2 & \frac{1}{105}l_1^2 & 0 & -\frac{1}{140}l_1^2 & 0 & 0 & 0 \\ & & \frac{1}{3} & 0 & 0 & 0 & 0 \\ & & & \frac{1}{105}l_1^2 & 0 & 0 & 0 \\ & \text{Symmetric} & & & 0 & 0 & 0 \\ & & & & & 0 & 0 \\ & & & & & & 0 \end{bmatrix}$$

$$[M_2] =$$

$$\rho_1 l_2 \begin{bmatrix} l_1^2 + l_1 l_2 + \frac{1}{3} l_2^2 + l_1 u_2 + \frac{1}{3} l_2 u_2 + l_1 u_3 + \frac{2}{3} l_2 u_3 + \frac{1}{3} u_2^2 + \frac{1}{3} u_2 u_3 + \frac{1}{105} l_2^2 \theta_2^2 + \frac{13}{210} l_2 \theta_2 v_3 - \frac{1}{70} l_2^2 \theta_2 \theta_3 + \frac{1}{3} u^2 + \frac{13}{35} v_3^2 - \frac{11}{105} l_2 v_3 \theta_3 + \frac{1}{105} l_2^2 \theta_3^2 & 0 & -\frac{1}{60}(3l_2\theta_2 + 9v_3 - 2l_2\theta_3) & \frac{1}{60} l_2 (2l_2 + 5l_1 + 3u_2 + 2u_3) & -\frac{1}{60}(2l_2\theta_2 + 21v_3 - 3l_2\theta_3) & \frac{1}{20}(7l_2 + 10l_1 + 3u_2 + 7u_3) & -\frac{1}{60} l_2 (3l_2 + 5l_1 + 2u_2 + 3u_3) \\ 0 & 0 & 0 & 0 & 0 & 0 \\ & \frac{1}{3} & 0 & \frac{1}{6} & 0 & 0 \\ & & \frac{1}{105} l_2^2 & 0 & \frac{13}{420} l_2 & -\frac{1}{140} l_2^2 \\ & \text{Symmetric} & & \frac{1}{3} & 0 & 0 \\ & & & & \frac{13}{35} & -\frac{11}{210} l_2 \\ & & & & & \frac{1}{105} l_2^2 \end{bmatrix}$$

$$[M_3] = \rho_2 l_3 \begin{bmatrix} 1 & 0 & \frac{1}{2}(l_3 + u_5)\sin\alpha_2 - \frac{1}{144} l_3 (\theta_4 - \theta_5)^2 \cos\alpha_2 & -\frac{1}{12} l_3 \sin\alpha_2 & \frac{1}{12}\cos\alpha_2 & 0 \\ & 1 & \frac{1}{2}(l_3 + u_5)\cos\alpha_2 - \frac{1}{12} l_3 (\theta_4 - \theta_5)\sin\alpha_2 & \frac{1}{12} l_3 \cos\alpha_2 & \frac{1}{12}\sin\alpha_2 & 0 \\ & & \frac{1}{210}\left(70 l_3^2 + 2\theta_4^2 l_3^2 - 3 l_3^2 \theta_4 \theta_5 + 140 l_3 u_5 + 70 u_5^2 + 2\theta_5^2 l_3^2\right) & \frac{1}{30} l_3 (l_3 + u_5) & -\frac{1}{60} l_3 (2\theta_4 - 3\theta_5) & 0 \\ & & & \frac{1}{105} l_3^2 & 0 & 0 \\ & & \text{Symmetric} & & \frac{1}{3} & 0 \\ & & & & & 0 \end{bmatrix}$$

A.2 Jacobian matrices and their time derivatives

$$[J_1] = \begin{bmatrix} -(l_1+u_2)\sin\alpha_1 & 0 & \cos\alpha_1 & 0 & 0 & 0 & 0 & -1 & 0 & 0 & 0 & 0 & 0 \\ (l_1+u_2)\cos\alpha_1 & 0 & \sin\alpha_1 & 0 & 0 & 0 & 0 & 0 & -1 & 0 & 0 & 0 & 0 \\ 0 & 0 & 0 & 0 & 0 & 0 & 0 & 1 & 0 & -(l_3+u_5)\sin\alpha_2 & 0 & \cos\alpha_2 & 0 \end{bmatrix}$$

$$[\dot{J}_1] = \begin{bmatrix} -(l_1+u_2)\dot{\alpha}_1\cos\alpha_1 - \dot{u}_2\sin\alpha_1 & 0 & -\dot{\alpha}_1\sin\alpha_1 & 0 & 0 & 0 & 0 & 0 & 0 & 0 & 0 & 0 & 0 \\ -(l_1+u_2)\dot{\alpha}_1\sin\alpha_1 + \dot{u}_2\cos\alpha_1 & 0 & \dot{\alpha}_1\cos\alpha_1 & 0 & 0 & 0 & 0 & 0 & 0 & 0 & 0 & 0 & 0 \\ 0 & 0 & 0 & 0 & 0 & 0 & 0 & 0 & 0 & -(l_3+u_5)\dot{\alpha}_2\cos\alpha_2 - \dot{u}_5\sin\alpha_2 & 0 & -\dot{\alpha}_2\sin\alpha_2 & 0 \end{bmatrix}$$

$$[J_2] = \begin{bmatrix} -(l_1+u_2)\sin\alpha_1 & 0 & \cos\alpha_1 & 0 & 0 & 0 & 0 & -1 & 0 & 0 & 0 & 0 & 0 \\ (l_1+u_2)\cos\alpha_1 & 0 & \sin\alpha_1 & 0 & 0 & 0 & 0 & 0 & -1 & 0 & 0 & 0 & 0 \\ 0 & 0 & 0 & 0 & 0 & 0 & 0 & 1 & 0 & -(l_3+u_5)\sin\alpha_2 & 0 & \cos\alpha_2 & 0 \\ 0 & 0 & 0 & 0 & 0 & 0 & 0 & 0 & 1 & (l_3+u_5)\cos\alpha_2 & 0 & \sin\alpha_2 & 0 \end{bmatrix}$$

$$[\dot{J}_2] = \begin{bmatrix} -(l_1+u_2)\dot{\alpha}_1\cos\alpha_1 - \dot{u}_2\sin\alpha_1 & 0 & -\dot{\alpha}_1\sin\alpha_1 & 0 & 0 & 0 & 0 & 0 & 0 & 0 & 0 & 0 & 0 \\ -(l_1+u_2)\dot{\alpha}_1\sin\alpha_1 + \dot{u}_2\cos\alpha_1 & 0 & \dot{\alpha}_1\cos\alpha_1 & 0 & 0 & 0 & 0 & 0 & 0 & 0 & 0 & 0 & 0 \\ 0 & 0 & 0 & 0 & 0 & 0 & 0 & 0 & 0 & -(l_3+u_5)\dot{\alpha}_2\cos\alpha_2 - \dot{u}_5\sin\alpha_2 & 0 & -\dot{\alpha}_2\sin\alpha_2 & 0 \\ 0 & 0 & 0 & 0 & 0 & 0 & 0 & 0 & 0 & -(l_3+u_5)\dot{\alpha}_2\sin\alpha_2 + \dot{u}_5\cos\alpha_2 & 0 & -\dot{\alpha}_2\cos\alpha_2 & 0 \end{bmatrix}$$

$$[J_3] = \begin{bmatrix}
-(l_1+u_2)\sin\alpha_1 & 0 & \cos\alpha_1 & 0 & 0 & 0 & 0 & -1 & 0 & 0 & 0 & 0 & 0 \\
(l_1+u_2)\cos\alpha_1 & 0 & \sin\alpha_1 & 0 & 0 & 0 & 0 & 0 & -1 & 0 & 0 & 0 & 0 \\
0 & 0 & 0 & 0 & 0 & 0 & 0 & 1 & 0 & -(l_3+u_5)\sin\alpha_2 & 0 & \cos\alpha_2 & 0 \\
0 & 1 & 0 & 0 & 0 & 0 & 0 & 0 & 0 & 0 & 0 & 0 & 0 \\
0 & 0 & 1 & 0 & 0 & 0 & 0 & 0 & 0 & 0 & 0 & 0 & 0 \\
0 & 0 & 0 & 1 & 0 & 0 & 0 & 0 & 0 & 0 & 0 & 0 & 0 \\
0 & 0 & 0 & 0 & 1 & 0 & 0 & 0 & 0 & 0 & 0 & 0 & 0 \\
0 & 0 & 0 & 0 & 0 & 1 & 0 & 0 & 0 & 0 & 0 & 0 & 0 \\
0 & 0 & 0 & 0 & 0 & 0 & 1 & 0 & 0 & 0 & 0 & 0 & 0 \\
0 & 0 & 0 & 0 & 0 & 0 & 0 & 0 & 0 & 0 & 1 & 0 & 0 \\
0 & 0 & 0 & 0 & 0 & 0 & 0 & 0 & 0 & 0 & 0 & 1 & 0 \\
0 & 0 & 0 & 0 & 0 & 0 & 0 & 0 & 0 & 0 & 0 & 0 & 1
\end{bmatrix}$$

$$[\dot{J}_3] = \begin{bmatrix}
-(l_1+u_2)\dot{\alpha}_1\cos\alpha_1 - \dot{u}_2\sin\alpha_1 & 0 & -\dot{\alpha}_1\sin\alpha_1 & 0 & 0 & 0 & 0 & 0 & 0 & 0 & 0 & 0 & 0 \\
-(l_1+u_2)\dot{\alpha}_1\sin\alpha_1 + \dot{u}_2\cos\alpha_1 & 0 & \dot{\alpha}_1\cos\alpha_1 & 0 & 0 & 0 & 0 & 0 & 0 & 0 & 0 & 0 & 0 \\
0 & 0 & 0 & 0 & 0 & 0 & 0 & 1 & 0 & -(l_3+u_5)\dot{\alpha}_2\cos\alpha_2 - \dot{u}_5\sin\alpha_2 & 0 & -\dot{\alpha}_2\sin\alpha_2 & 0 \\
0 & 0 & 0 & 0 & 0 & 0 & 0 & 0 & 0 & 0 & 0 & 0 & 0 \\
0 & 0 & 0 & 0 & 0 & 0 & 0 & 0 & 0 & 0 & 0 & 0 & 0 \\
0 & 0 & 0 & 0 & 0 & 0 & 0 & 0 & 0 & 0 & 0 & 0 & 0 \\
0 & 0 & 0 & 0 & 0 & 0 & 0 & 0 & 0 & 0 & 0 & 0 & 0 \\
0 & 0 & 0 & 0 & 0 & 0 & 0 & 0 & 0 & 0 & 0 & 0 & 0 \\
0 & 0 & 0 & 0 & 0 & 0 & 0 & 0 & 0 & 0 & 0 & 0 & 0 \\
0 & 0 & 0 & 0 & 0 & 0 & 0 & 0 & 0 & 0 & 0 & 0 & 0 \\
0 & 0 & 0 & 0 & 0 & 0 & 0 & 0 & 0 & 0 & 0 & 0 & 0 \\
0 & 0 & 0 & 0 & 0 & 0 & 0 & 0 & 0 & 0 & 0 & 0 & 0
\end{bmatrix}$$